UNIVERSITAT DE BARCELONA

The possible link between high glucose-induced PKCβ expression and the appearance of GLP-1 resistance in endothelial cells

Valeria De Nigris

Universitat de Barcelona

FACULTAT DE MEDICINA

THE POSSIBLE LINK BETWEEN HIGH GLUCOSE-INDUCED PKCβ EXPRESSION AND THE APPEARANCE OF GLP-1 RESISTANCE IN ENDOTHELIAL CELLS

Thesis submitted by
Valeria De Nigris

To qualify for the Title of
Ph.D. from the University of Barcelona

Institut
D'Investigacions
Biomèdiques
August Pi i Sunyer

diabetes obesity Research

Doctoral Program in Biomedicine

This thesis has been carried out under the supervision of
the **Director Prof. Antonio Ceriello**,
the **Co-Director Dr. Gemma Pujadas i Rovira**
and the **Tutor Prof. Ramon Gomis de Barbarà**
at the Diabetes and Obesity Laboratory
of the *Institut d'Investigacions Biomèdiques August Pi I Sunyer* (IDIBAPS).

Prof. Antonio Ceriello **Dr. Gemma Pujadas** **Prof. Ramon Gomis**

Valeria De Nigris

Barcelona, December 2015

A Papà, ti vedo sorridere insieme a me. Sempre.
A Mamma, a te devo questo viaggio meraviglioso che è la vita.

È l'unica parte di questa tesi che scrivo in italiano. Mi perdonerete, ma non posso fare altrimenti: sono sempre stata convinta che i sentimenti, quelli che vengono fuori dal cuore, non possono che essere espressi nella propria lingua. Sono sicura che tutti comprenderete i miei pensieri, d'altronde, dopo quattro anni trascorsi insieme a Valeriuccia "la italianina", non potete non aver appreso un po' di italiano!

Questa tesi rappresenta la realizzazione di un'altra importante tappa della mia vita, il punto di arrivo di un percorso che mi ha arricchita tanto, non solo professionalmente, ma anche umanamente.

Il mio primo ringraziamento lo devo al Prof. Antonio Ceriello, il mio "caro Prof", che non è solo un grande Capo, ma in questi anni si è rivelato per me molto di più: ha saputo aiutarmi e consigliarmi nelle mie scelte professionali così come in quelle personali. È grazie al suo costante supporto che posso proseguire i miei studi di medicina, con tanti sacrifici, ma allo stesso tempo tante soddisfazioni.

Un ringraziamento particolare va al Prof. Ramón Gomis, non solo un grande ricercatore, ma anche un grande medico e soprattutto un grande uomo.

Alla Doctora Anna Novials. Alla sua immensa disponibilità, accompagnata sempre dall'allegria che la contraddistingue.

Alla Doctora Gemma Pujadas. Senza di lei non avrei scritto questa tesi. Sempre presente, attenta, professionale, rigorosa e scrupolosa, ho appreso molto da lei e dalla passione che quotidianamente profonde nel suo lavoro.

Alla Dottoressa Lucia La Sala, al suo impegno nel cercare di fare sempre meglio e alla sua vitalità.

A Margherita, Amica con la A maiuscola a Barcellona, a Benevento, a Venturina e ovunque andremo.

Ai Principal Investigators del gruppo di Diabete e Obesità, i Dottori: Marc, Rosa, Marcelina e Juan Marc.

Al Doctor Pablo García Rovez e al Doctor Carles Lerín.

Alla "Familia Barcelonina", ai miei colleghi e amici passati e presenti:

- Joel, Mercé O., Carlitos, Sara deP. e Julia, compagni di caffè e confidenze extra-lab;
- Elena, Marta, Didi, Lisa, Elaine e Liz, compagne di vermouth e afterwork all'Hyde;
- Albuki, Montse, Gema, Lidia, Ainhoa, Yaiza, Sara C., Joan, Hugo e AnaLu, Rita, Joana, Mercé M. e Pau;
- Alicia, Iñigo e Sara, i miei "Claretines";
- Xavi, Vane, Elena, Loris e Meritxell, Mar, Lorenzo e Irene, i miei "ex-vicini";
- Francesco, il nuovo arrivato che ha conquistato subito tutti con i cornetti al lab meeting e la sua amatriciana!

Ad Alba e Marc, compagni di mille avventure. Mi sono stati vicini nei momenti belli e in quelli bui, vivendo insieme a me i sorrisi e gli sguardi tristi di questi intensi quattro anni.

A Victoria e ai suoi "No puedo!". A Valeria, il mio alter-ego. A Cristina, chi ha detto che l'amicizia vera non può nascere anche a 28 anni suonati?!

A Franceca e Chiara, che hanno saputo starmi accanto come sorelle. A Laura.

Ai miei amici di sempre: Giangi, Enzo e Fabiola. Dopo tutti questi anni, mi guardo indietro e capisco che ci sono stati sempre. La distanza non ha mai rappresentato un ostacolo. Siamo lontani, ma non ci siamo mai persi.

A Olga. Energia per ogni nuova giornata nelle nostre parole, nella grinta di ricominciare, di rivoltare il mondo, di sorridere alla vita. Chilometri di distanza da annullare per un abbraccio la cui intensità ci dona la forza di attendere per mesi il prossimo. E la sicurezza, l'unica certezza: quella di esserci per sempre. Io per te. Tu per me. Senza tempo, senza distanza.

A Vittorio. Mi ha insegnato che la Medicina non è una professione, ma una scelta di vita. Mi ha insegnato il valore di ESSERE medico, che non è FARE il medico.

A tutta la banda dei cugini, matti e preziosi. A quelli di sempre, Nina, Mari, Vale, Marina, Mirella, Antonella, Rocco e Debora, e a quelli "acquisiti", Marco, Gigi, Ivan, Fabio, Andrea, Antonio e Stefano.

A Maurizio e Marilena, sempre presenti e vicini, anche se a 1500 km di distanza.

Ad Alberto. A questa vita, che non smette mai di stupirmi. A Vueling, che da qualche tempo odio un po' meno. Agli Aerobus.

Alla mia Famiglia, il mio punto di partenza e di arrivo, il mio luogo di rifugio, la mia costante fonte di amore, di gioie e di sorrisi. Nonostante tutto.

Ad Angelo, il mio guerriero della luce. Hai dovuto imparare a crescere in fretta, più di me.

A Mamma, donna straordinariamente straordinaria. Dai gioia di vivere con il tuo sorriso, nonostante tutto. Tra tante cose, mi hai insegnato quella più importante: "mangiare a morsi" questa vita, che è il bene più prezioso che ho.

A Papà. Ti sento, sei qui con me.

INDEX

ABBREVIATIONS

2 hours post load plasma glucose	2-h PG
2’,7’-Dichlorofluorescein diacetate	H_2DCFDA
3-[4,5-dimethylthiazol-2-yl]-2,5- diphenyltetrazolium bromide; thiazolyl blue	MTT
5' adenosine monophosphate-activated protein kinase	AMPK
5-bromodeoxyuridine	BrdU
α-tubulin	TUBA
β-actin	ACTB
β-arrestin isoform 1	Barr1
β-arrestin isoform 2	Barr2
Activating transcription factor 4	ATF4
Activating transcription factor 6	ATF6
Adenylate cyclase	AC
Advanced glycation end-products	AGEs
American Diabetes Association	ADA
American Heart Association	AHA
Angiotensin II	Ang II
Antioxidant responsive elements	ARE
Apoptosis signalling kinase 1	ASK-1
Ataxia telangiectasia mutated	ATM
Atypical PKC	aPKC
Bovine serum albumin	BSA
Breast cancer susceptibility 1	BRCA1
C/EBP homologous protein	CHOP
cAMP response element-binding protein	CREB
Carbon monoxide	CO
Cardiovascular disease	CVD
Catalase	CAT
Central nervous system	CNS
Clathrin-coated pits	CCPs
Clathrin-coated vesicles	CCVs
Complementary DNA	cDNA
Conventional PKC	cPKC
Cultured aortic endothelial cells	CAECs
Cyclic adenosine monophosphate	cAMP
Cyclin-dependent kinase inhibitor 1A	CDKN1A/p21
Cyclin-dependent kinase inhibitor 1B	CDKN1B/p27
Cytosolic copper/zinc SOD	Cu/ZnSOD
Diacylglyceride	DAG
Dimethyl sulfoxide	DMSO
Dipeptidyl dipeptidase-4	DPP-4
Double-strand DNA	dsDNA
Dulbecco's Phosphate-Buffered Saline	DPBS
Electron transport chain	ETC
Electrophile response elements	EpRE
Endoplasmic reticulum	ER
Endothelial cells	ECs
Endothelial nitric oxide synthase	eNOS
Endothelial progenitor cells	EPCs
Endothelin 1	ET-1
Endothelium-derived hyperpolarizing factor	EDHF
Endothelium-derived relaxing factor	EDRF
Epidermal growth factor receptor	EGRP
ER-associated degradation	ERAD
Eukaryotic translation initiation factor 2	eIF2a
Exchange factor directly activated by cAMP	EPAC
Extracellular SOD	ecSOD
Fasting plasma glucose	FPG
Fetal Bovine Serum	FBS
Flavin adenine dinucleotide	FAD
Flavin mononucleotide	FMN
Fluoroscein isothiocyanate	FITC
Forkhead box O	FOXO
Free fatty acids	FFAs

Fructose-2,6-bisphosphate	Fru-2,6-P_2
G protein receptor kinases	GRKs
G protein-coupled receptor	GPCR
G protein-coupled receptor kinase	GRK
Gentamicin/Amphotericin-B	GA
Gestational diabetes mellitus	GDM
GIP receptor	GIPR
Glicentin-related polypeptide	GRPP
Glomerular endothelial cells	RGECs
GLP-1 receptor	GLP-1R
Glucagon	GLUC
Glucagon-like peptide 1	GLP-1
Glucose-dependent insulinotropic polypeptide	GIP
Glutamate–cysteine ligase	GCL
Glutaminase 2	GLS2
Glutamine fructose-6-phosphate amidotransferase	GFAT
Glutathione	GSH
Glutathione peroxidase	GPX
Glutathione S-transferase Mu1	GSTM1
Glutathione S-transferase	GST
Glycated hemoglobin	HbA1c
Glyceraldehyde 3-phosphate dehydrogenase	GAPDH
Growth arrest and DNA damage-inducible protein	GADD34
GSH synthase	GSS
Heme oxygenase	HMOX-1
High glucose	HG
Human aortic endothelial cells	HAECs
Human coronary artery endothelial cells	HCAECs
Human Epidermal Growth Factor	hEGF
Human recombinant Fibroblast Growth Factor-Beta	hFGF-b
Human umbilical vein endothelial cells	HUVECs
Hydrogen peroxide	H_2O_2
Hydroxyl radical	$OH^{\cdot}$
Hypochlorous acid	HOCl
Hypoxia-inducible transcription factor 1	HIF1
Immunoglobulin heavy chain binding protein/glucose-regulated protein of 78kDa	BiP/GRP78
Inducible nitric oxide synthase	iNOS
Inositol trisphosphate	IP_3
Inositol-requiring enzyme 1	IRE1
International Diabetes Federation	IDF
Intervening peptide-1	IP-1
Intervening peptide-2	IP-2
IRE1/X box binding protein-1	XBP-1
Jun-terminal kinase	JNK
Kelch-like ECH-associated protein 1	KEAP1
Laminin-β1	LMNB1
Lipid radicals	$LOO^{\cdot}$
Macrophage stimulating protein 1	MST1
Major proglucagon fragment	MPGF
Manganese	Mn
Maturity-onset diabetes of the young	MODY
Mitochondrial DNA	mtDNA
Mitochondrial ROS	mtROS
Mitogen-activated protein kinase	MAPK
NADPH Oxidase	NOX
NADPH:quinone oxidoreductase 1	NQO-1
Neuronal NOS	nNOS
Nitric oxide	NO
Non-insulin-dependent diabetes mellitus	NIDDM
Normal glucose	NG
Novel PKCs	nPKC
Nuclear factor erythroid 2-related factor 2	NRF2
Nuclear factor-κB	NF-κB

One-way analysis of variance	ANOVA
Oral glucose tolerance test	OGTT
Oxidative phosphorylation	OXPHOS
Oxidized glutathione disulphide	GSSG
Oxyntomodulin	OXM
Pentose phosphate pathway	PPP
Permanent neonatal diabetes	PNDM
Peroxiredoxin	PRX
Peroxynitrite	$ONOO^-$
Phosphatase and tensin homolog	PTEN
Phosphatidylinositol 4,5-bisphosphate	PIP_2
Phosphofructokinase 1	PFK1
Phosphoinositide 3-kinase	PI3K
Phospholipase C	PLC
PKC Diabetic Macular Edema Study	PKC-DMES
PKC-Diabetic Retinopathy Study	PKC-DRS
PKC-Diabetic Retinopathy Study 2	PKC-DRS2
PKR-like eukaryotic initiation factor 2a kinase	PERK
Platelet-derived growth factor	PDGF
Poly ADP ribose polymerase	PARP
Polyacrylamide gel electrophoresis	PAGE
Prostaglandin H2	PGH2
Protein kinase A	PKA
Protein kinase C	PKC
Protein kinase G	PKG
Protein phosphatase 1	PP1
PTEN-induced putative kinase	PINK1
Reactive oxygen species	ROS
Regulated IRE1-dependent decay	RIDD
Retinal blood flow	RBF
Reverse transcription	RT
Ruboxistaurin	RBX
Sarcoendoplasmic reticulum Ca^{2+} ATPase	SERCA
Site 1 protease	S1P
Site 2 protease	S2P
Smooth muscle cells	SMCs
Soluble guanylate cyclase	sGC
Sorbitol dehydrogenase	SDH
Standard error of the mean	SEM
Superoxide	$\cdot O_{2^-}$
Superoxide Dismutase-1	SOD1
Superoxide Dismutase-2	SOD2
Tetrahydrobiopterin	BH_4
Tetramethylrhodamine	TRITC
Thioredoxin	TXN/TRX
Thioredoxin interacting protein	TXNIP
Thioredoxin reductase	TXNRD
Thromboxane A2	TXA2
TP53-induced glycolysis and apoptosis regulator	TIGAR
Transforming growth factor-β	TGF-β
Transient neonatal diabetes	TNDM
Tribbles homolog 3	TRB3
Tricarboxylic acid	TCA
Tumor necrosis factor receptor-associated factor 2	TRAF2
Type 1 diabetes mellitus	T1DM
Type 2 diabetes mellitus	T2DM
UDP-glucuronosyltransferases	UGTs
Unfolded Protein Response	UPR
Vascular endothelial growth factor	VEGF
Vascular endothelial growth factor A	VEGFA
Vascular smooth muscle cells	VSMCs
Very low density lipoprotein	VLDL
Wolfram syndrome 1	WFS1

SUMMARY

Introduction. It has been demonstrated that Glucagon-like peptide-1 (GPL-1) has a protective effect on endothelial cells. GLP-1 improves endothelial function in diabetes, however the mechanisms underlying the GLP-1 protective effects have not yet been fully elucidated. Additionally, it has been proposed that GLP-1 could restore high glucose - endoplasmic reticulum (ER) stress induction. Recent evidences claim a resistance of GLP-1 action that has been shown in pancreatic β-cells of diabetic patients. A proposed mechanism to explain this resistance to the GLP-1 action in diabetes is the activation of PKCβ, induced by hyperglycaemia, which is able to reduce the expression of GLP-1 receptor.

Aim. The aim of this thesis project was to decipher if GLP-1 acute treatment is able to counteract chronic high glucose-induced damage in Human umbilical Vein Endothelial cells (HUVECs).

Methods. In this study HUVECs were cultured for 21 days under normal glucose (5mmol/L, NG) or high glucose (25mmol/L glucose, HG) concentrations. GLP-1 and Ruboxistaurin were added alone or in combination, 1 hour before cell harvesting. Analysis of GLP-1 receptor protein levels as well as of gene expression of different ER stress-related genes, proliferation markers, antioxidant cell response-related genes and PKA subunits was performed. ROS production was also measured in HUVECs exposed to mentioned treatments.

Results. GLP-1 receptor expression was reduced in HUVECs exposed to chronic high glucose concentrations and it was partially restored after treatment with the chemical PKCβ specific inhibitor, Ruboxistaurin. GLP-1, added as an acute treatment in endothelial cells, had the capacity to induce the expression of detoxifying enzymes Nrf2 targets, to increase transcript levels of scavenger genes, to attenuate the high glucose-induced PKA subunits expression, ER stress and also the apoptotic phenotype of HUVECs only when high glucose-induced PKCβ overexpression was reduced by Ruboxistaurin. In the same direction, ROS production induced by high glucose was reduced by GLP-1 in the presence of PKCβ inhibitor.

Conclusions. This study suggests that PKCβ increase, induced by high glucose, could have a role in endothelial GLP-1 resistance, reducing GLP-1 receptor levels and disrupting GLP-1 canonical pathway.

Keywords. Diabetes, high glucose, GLP-1, PKCβ, endothelial dysfunction, incretin resistance.

INTRODUCTION

1. Diabetes Mellitus

Diabetes mellitus is a complex metabolic disorder characterized by defects in the body's ability to control glucose and insulin homeostasis. It is a global epidemic, with significant social and economic consequences both for individuals and overall public health. The *International Diabetes Federation* (IDF) estimates that 382 million people worldwide currently have diabetes and predicts that 592 million will suffer from the disease in 2035 (Aguiree et al. 2013) (Figure 1).

Diabetes encompasses a heterogeneous group of metabolic disorders with the common features of hyperglycaemia and lack of insulin compensation in peripheral tissues (Canivell and Gomis 2014). Lack of insulin compensation is a consequence of a defect in insulin secretion, an impaired insulin action or both. This is accompanied by an alteration in the metabolism of carbohydrates, fats and proteins, and an increase in the risk of heart disease, stroke and other cardiovascular complications (Drouin et al. 2013).

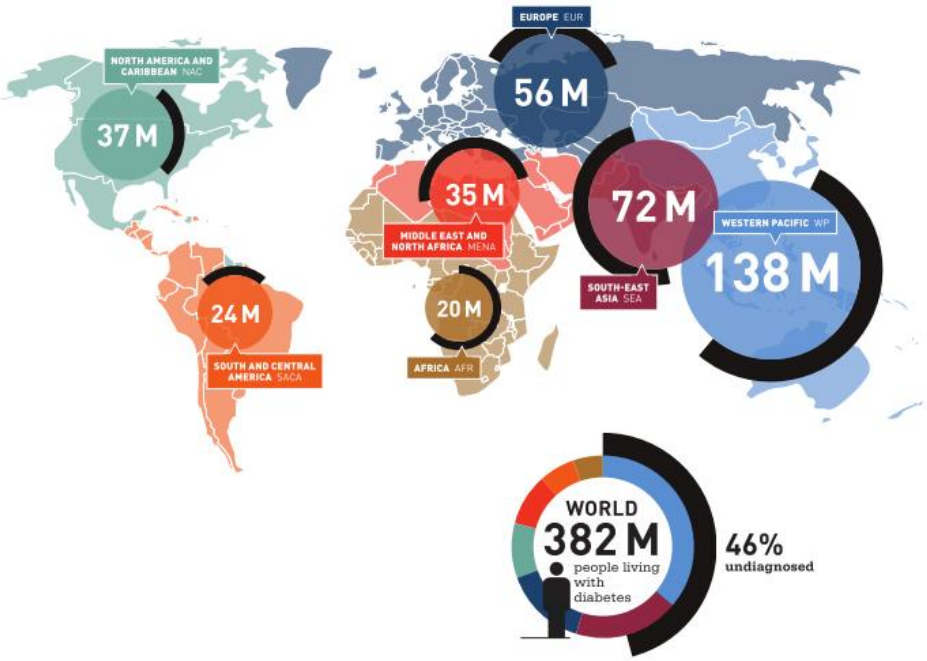

Figure 1: Number of worldwide people with diabetes. IDF's most recent estimation indicating that 382 million people have diabetes and the number of people with the disease will rise beyond 592 million in less than 25 years. Here there is a representation of the distribution of diabetic people in the world (Aguiree et al. 2013).

Hyperglycaemia is the hallmark of all forms of diabetes and represents the condition in which an excessive amount of glucose circulates in plasma. Chronic hyperglycaemia is associated with failure of different organs, especially eyes, kidney, nerves, heart and blood vessels (Laakso 1999).

Ancient literature from Egypt and India described the disease as it was easily identifiable because "a patient's urine attracted ants" (Ahmed 2002). More than two millennia later, monitoring glycemic status continues to be central for the clinical management. Nowadays scientific and medical world is in concordance with the idea that a subject with a consistent range between 100 and 126 mg/dl of blood glucose levels is considered hyperglycemic, while diabetes is diagnosed for levels of fasting plasma glucose (FPG) > 7mmol/l (126 mg/dl) or 2 hours post load plasma glucose (2-h PG) > 11.1mmol/l (200mg/dl) during a 75g oral glucose tolerance test (OGTT) (Drouin et al. 2009). A maintained glucose level higher than 11.1mmol/l could be very dangerous for human body even if

symptoms may not start to become noticeable before reaching higher values such as 15-20mmol/l (250-300mg/dl) (Drouin et al. 2009; T. J. Wang et al. 2011).

For clinical diagnosis and control of diabetic subjects, another very useful parameter is the glycated hemoglobin (HbA1c) (Kesavadev et al. 2014; Selvin et al. 2011). It is a form of hemoglobin that is measured primarily to identify the plasma glucose concentration average over prolonged periods of time. It is formed in a non-enzymatic glycation pathway by hemoglobin's exposure to plasma glucose. Normal levels of glucose produce a normal amount of glycated hemoglobin, and when the average amount of plasma glucose increases, the fraction of glycated hemoglobin increases in a predictable way. In diabetes mellitus, higher amounts of glycated hemoglobin, indicating poorer control of blood glucose levels, have been associated with cardiovascular disease, nephropathy, and retinopathy. So, a tight control of glucose levels is associated with reduced incidence (Kesavadev et al. 2014) and slower progression of diabetes-related complications, myocardial infarction and stroke (Stratton et al. 2000). Because monitoring HbA1c in diabetic patients may improve outcomes, the *American Diabetes Association* (ADA) released guidelines recommending that target HbA1c for people with diabetes should be less than 7% (53mmol/mol) (Kdoqi 2007).

Diabetes mellitus is classified into three broad categories: type 1, type 2, and gestational diabetes (Figure 2). Finally there are "other specific types" (Aguiree et al. 2013; Drouin et al. 2009) which are a collection of a few dozen individual causes.

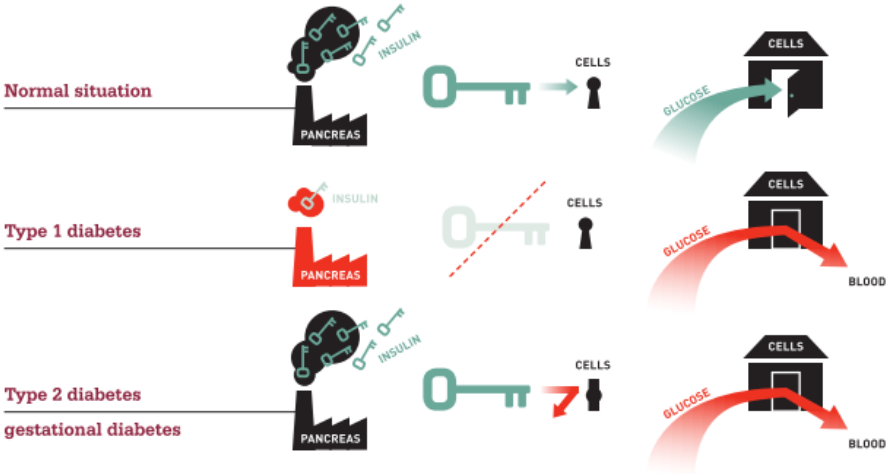

Figure 2: The three main types of diabetes. Type 1 diabetes, the result of an autoimmune process, needs insulin therapy. In type 2 diabetes, a defect in insulin action occurs and subjects affected can go unnoticed and undiagnosed for years. Gestational diabetes can lead to serious risks to the mother/infant and increase the risk for developing type 2 diabetes later in life (Aguiree et al. 2013).

1.1. Type 1 Diabetes Mellitus

Previously encompassed by the terms “insulin-dependent diabetes” or “juvenile-onset diabetes”, type 1 diabetes mellitus (T1DM) accounts for only 5%-10% of all diabetes cases (Canivell and Gomis 2014; Drouin et al. 2013) and its diagnosis is made commonly in childhood (Craig, Hattersley, and Donaghue 2009). It results from a cellular-mediated autoimmune destruction of the insulin-producing pancreatic β-cells of the islets of Langerhans and it is characterized by a lack of insulin production, rendering patients absolutely dependent on exogenous insulin (Canivell and Gomis 2014).

Due to the lack of insulin, subjects with T1DM have an impaired glucose homeostasis and peripheral tissues are not able to metabolize the glucose. The liver in turn produces more glucose through the gluconeogenesis and gycogenolysis, increasing hyperglycaemia, as well as it starts to metabolize others substrates, such as free fatty acids. This metabolic dysregulation causes ketoacidosis and other secondary complications due to chronic hyperglycaemia.

In order to maintain a proper glucose homeostasis and metabolism, T1DM patients require lifelong insulin as a treatment. Episodes of hypoglycaemia can occur due to insulin treatment, so that a strict control of injected insulin and glycemic blood levels is needed (Canivell and Gomis 2014).

1.2. Type 2 Diabetes Mellitus

Type 2 Diabetes Mellitus (T2DM), also known as “non-insulin-dependent diabetes mellitus” (NIDDM) or “adult-onset diabetes”, represents the most common form of the disease, accounting for 90-95% of individuals with diabetes, usually with onset in adult (Alberti and Zimmet 1998). It is a metabolic disorder characterized by high blood glucose levels, insulin resistance and finally a relative insulin deficiency, as opposed to the absolute deficiency observed in T1DM (DeFronzo 2004).

At least initially, and often throughout their lifetime, if they are well-controlled, these individuals do not need insulin treatment to survive. When the diagnosis of T2DM becomes clear, patients are initially managed to decrease hyperglycaemia by modifications in diet and lifestyle. If these regulations are not sufficient to reduce blood glucose levels, sulfonylureas and incretin analogues such as exendin-4 can be used to potentiate insulin secretion during the early development of disease. Insulin resistance may also be improved using thiazolinediones or metformin. Only in advanced stages, when disease has progressed to β-cell failure, patients will need insulin injections and a strict glycemic control (Ferrannini and DeFronzo 2015; Inzucchi et al. 2012). There are many possible different causes of this form of diabetes. T2DM has a strong genetic component but it is also influenced by lifestyle factors, such as age, physical activity, pregnancy and obesity. Obesity-associated insulin resistance is one of the major risk factors for developing T2DM (Drouin et al. 2013).

During disease progression different tissues are affected becoming insulin-resistant. In skeletal muscle of these individuals, the insulin is not able to stimulate glucose uptake after a carbohydrate meal and this results in postprandial hyperglycaemia. The failure of insulin to exert its “hypoglycaemizant effect” in skeletal muscle is considered the first alarm of developing T2DM (DeFronzo 2004). In adipose tissue, insulin resistance causes increased lipolysis and fatty acid release. Once released, fatty acids decrease the ability of insulin to suppress glucose production in the liver and, at the same time, allow a constant increase in insulin-stimulated fatty acid synthesis. This deregulation of carbohydrates and lipids acts as a vicious circle accelerating the progression of insulin resistance. At first, pancreatic β-cells have the ability to compensate the insulin resistant state by increasing basal and postprandial insulin secretion. The problem is that in this way they contribute to aggravate the insulin resistance condition. As consequence of their own effects, β-cells can no longer compensate and became enable to respond appropriately to glucose. This ultimately leads to the deterioration of glucose homeostasis and the development of glucose intolerance. Adipose tissue and liver continue to generate fatty acids, liver also overproduces glucose in an unregulated manner and the pancreatic β-cells undergo to a progressive decompensation. This pattern of physiological abnormalities in skeletal muscle, adipose tissue, liver and pancreas results in the late stages of the disease (Saltiel and Kahn 2001).

1.3. Other forms of diabetes

1.3.1. Gestational diabetes

Gestational diabetes mellitus (GDM) is formally defined as any degree of glucose intolerance with onset or first recognition during pregnancy (Drouin et al. 2013). A woman is diagnosed with gestational diabetes when glucose intolerance continues beyond 24–28 weeks of gestation (Gupta et al. 2015).

Although the precise mechanisms underlying gestational diabetes remain unknown, the hallmark of GDM is the increased insulin resistance, which normally occurs in the second trimester of pregnancy and is mediated by hormones and increased fat deposits that are accumulated during pregnancy. These and other factors are thought to interfere with the action of insulin in binding its receptor (Durnwald 2015).

1.3.2. The maturity-onset diabetes of the young and others

There is a subset of diabetes attributable to single gene mutations that affect β-cell development or cause severe β-cell dysfunction (Drouin et al. 2013). These types of diabetes are: maturity-onset diabetes of the young (MODY), permanent neonatal diabetes (PNDM) and transient neonatal diabetes (TNDM). PNDM and TNDM are diagnosed within the first three months of life (1/400.000 births) (Craig, Hattersley, and Donaghue 2009), whereas MODY is developed prior 25 years and has a prevalence of 2% of diagnosed diabetes patients. Different types of MODY are classified depending on the mutated gene, being the most common forms GCK-MODY (MODY2) and HNF1α-MODY (MODY3) due to mutations in the GCK and HNF1A genes, respectively.

Diabetes can also be caused by medications, endocrinopathies and defects of the exocrine pancreas. Glucocorticoids and other immunosuppressive agents are used drugs known to cause diabetes. Cushing syndrome, acromegaly and hyperthyroidism among others are endocrinopathies in which diabetes may be developed too (Nathan 2015).

2. Diabetes mellitus and cardiovascular disease

There is a strong correlation between diabetes and cardiovascular disease (CVD) (Bloomgarden 2008; Laakso 1999). All forms of diabetes are actually characterized by chronic hyperglycaemia but also by the development of specific microvascular and macrovascular complications (Snell-Bergeon and Wadwa 2012).

At microvascular level, diabetes can lead to serious diseases affecting retina, renal glomerulus and peripheral nerve. As a consequence of these microvascular complications, diabetes is a leading cause of blindness, end-stage renal disease and a variety of debilitating neuropathies (Aguiree et al. 2013). Diabetes is also associated with accelerated atherosclerotic macrovascular disease affecting arteries that supply the heart, brain and lower extremities. As a result, patients with diabetes have a much higher risk of ischemia, myocardial infarction, stroke, peripheral vascular disease and limb amputation (Aguiree et al. 2013).

It has been estimated that patients with T2DM have almost twice the risk of CVD of non-diabetic individuals after adjustment for other cardiovascular risk factors (Bloomgarden 2008) and, according to the *American Heart Association* (AHA), heart disease and stroke are the main cause of death and

disability among people with T2DM. The combination of the following conditions contributes to the risk for developing CVD in diabetic population, particularly in T2DM (http://www.heart.org/HEARTORG/Conditions/Diabetes/WhyDiabetesMatters/Cardiovascular-Disease-Diabetes_UCM_313865_Article.jsp):

- Hypertension: it has long been recognized as the major risk factor for cardiovascular disease. Studies report a positive association between hypertension and insulin resistance (Bloomgarden 2008).
- Hypercholesterolemia and hypertriglyceridemia: patients with diabetes often have unhealthy cholesterol levels (high LDL cholesterol, low HDL cholesterol and high triglycerides), potentiating premature coronary heart disease.
- Obesity: it is the main risk factor for cardiovascular disease and has been strongly associated with insulin resistance. Weight loss can improve cardiovascular risk, decreasing insulin concentration and increasing insulin sensitivity.
- Physical inactivity: it is another major risk factor for insulin resistance and cardiovascular disease. Exercising and losing weight can prevent or delay the onset of T2DM, reducing blood pressure and helping to reduce the risk for heart failure and stroke.
- Smoking: cigarettes smoking increase, whether or not diabetes disease, the risk for heart disease and stroke.

In synthesis, hypertension is considered the major modifiable risk factors for cardiovascular disease. Further modifiable risk factors include hypercholesterolaemia, obesity and those associated with low socioeconomic status, such as cigarette smoking and sedentary lifestyle (http://www.bhf.org.uk/research/statistics.aspx). Conversely, aging, family history of CVD, gender and ethnicity represent non-modifiable disease risk factors (Figure 3) (Dominiczak et al. 2005).

If the relative burden of CVD attributable to traditional risk factors, such as smoking, hypertension and hypercholesterolemia, has declined in recent years, findings, such as those from "The Framingham Heart Study", suggest that an increasing prevalence of T2DM has led to an increase in the proportion of CVD due to diabetes mellitus (Kannel and McGee 1979; Smith 2007), and these data are much more consistent if diabetes is associated with the traditional risk factors commented before: individuals with diabetes in combination with one or more of these risk factors are more likely to fall victim to CVD.

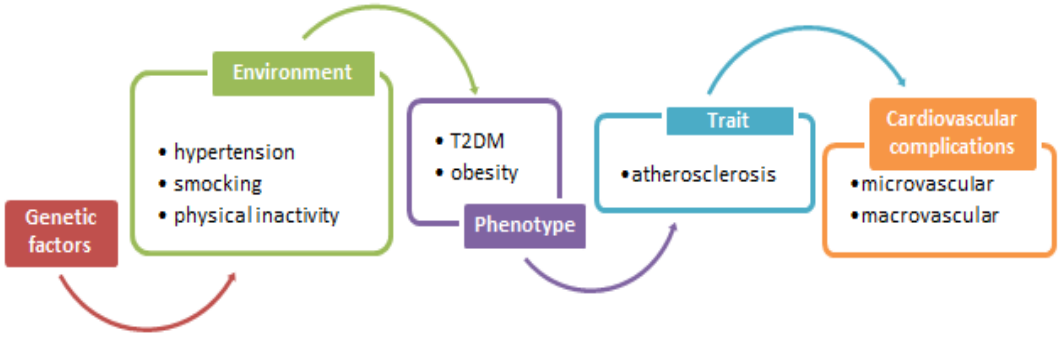

Figure 3: Cardiovascular disease risk factors. Multiple interactions between genetic and environmental factors result in the target organ damage characteristic of cardio-vascular disease. Adapted from Dominiczak et al. (Dominiczak et al. 2005)

3. Endothelial dysfunction in diabetic cardiovascular complications

A striking feature of diabetic cardiovascular complications is the appearance of accelerated atherosclerosis, which anatomically resembles atherosclerosis in non-diabetic individuals but is more extensive and occurs at an earlier age (Dominiczak et al. 2005). Substantial clinical and experimental evidence suggests that endothelial dysfunction is a crucial early step in the development of atherosclerosis (Tabit et al. 2010). Evidence also suggests that it participates in plaque progression and the clinical emergence of cardiovascular events (Basha et al. 2012).

3.1. Vascular endothelium

More than a trillion endothelial cells (ECs) line the luminal surface of the human vasculature, representing a critical interface between circulating blood and tissue. Originally considered to be simply a physical barrier, the endothelium is now recognized as an important endocrine organ and the fundamental component of normal vascular homeostasis, because it serves to maintain the anticoagulant, antiplatelet and fibrinolytic phenotypes of vascular cells (Bakker et al. 2009; Simsek et al. 2010; Tabit et al. 2010). In normal conditions, the endothelium plays a pivotal role in maintaining cardiovascular homeostasis by releasing a number of vasodilator and vasoconstrictor substances which act to regulate vascular tone, antiproliferation and antiaggregation, in addition to limiting increases in blood pressure, controlling tissue blood flow and inflammatory responses and maintaining blood fluidity. The endothelium releases these vasoactive substances in response to mechanical stimuli, such as pressure and shear stress, and various hormonal stimuli, such as insulin (Potenza et al. 2005).

The most important factor released by the endothelium is the vasodilator nitric oxide (NO), originally identified as endothelium-derived relaxing factor (EDRF) (Moncada and Higgs 2006a; Vanhoutte 2006; Xu and Zou 2009). Other endothelium-derived vasodilators include prostacyclin (Moncada et al. 1976), bradykinin, and an uncharacterized endothelium-derived hyperpolarizing factor (EDHF) (G. Chen, Suzuki, and Weston 1988). Prostacyclin acts synergistically with NO to inhibit platelet aggregation. Bradykinin stimulates release of NO, prostacyclin, and EDHF to inhibit platelet aggregation. Bradykinin also stimulates production of tissue plasminogen activator and thus may play an important role in fibrinolysis.

The endothelium also produces vasoconstrictor substances such as endothelin 1 (ET-1) that is recognized as the most potent endogenous vasoconstrictor (Yanagisawa et al. 1988), and also reactive oxygen species (ROS) (Xu and Zou 2009), prostaglandin H2 (PGH2), thromboxane A2 (TXA2), and angiotensin II (Ang II). Ang II is not only a vasoconstrictor but also a pro-oxidant that stimulates production of ET-1. ET-1 and Ang II promote proliferation of smooth muscle cells (SMCs) and in this way contribute to plaque formation. Large amounts of ET-1 are produced by activated macrophages and vascular smooth muscle cells (VSCMs), the cellular components of atherosclerotic plaques.

3.2. Endothelial dysfunction

Because the endothelium plays a key role in vascular homeostasis, damage to this cellular layer will disrupt the balance between vasoconstriction and vasodilation, initiating a number of events/processes that promote or exacerbate atherosclerosis (Tabit et al. 2010). These include endothelial permeabilization, platelet aggregation, leukocyte adhesion and cytokine production and

all these events lead to the pathological condition known as “endothelial dysfunction”. All forms of cardiovascular disease have been shown to be associated with some degree of endothelial dysfunction (Simsek et al. 2010; Tabit et al. 2010; Vanhoutte 2006; Xu and Zou 2009).

The term “endothelial dysfunction” was coined in the mid-eighties, following the major breakthrough by Furchgott and Zawadzki (Furchgott and Zawadzki 1980), and it was suggested that this condition could be an early marker of atherosclerosis (Jayakody et al. 1988). Since then, the term has been associated not only to hypertension or atherosclerosis, but also to a variety of physiological and pathophysiological processes including: aging, heart and renal failure, coronary syndrome, thrombosis, intravascular coagulation, inflammation, impaired glucose tolerance, insulin resistance, hyperglycaemia, obesity, hypercholesterolemia, including T1DM and T2DM.

At molecular level, endothelial dysfunction describes the situation when a shift in the equilibrium between vasodilator and vasoconstrictor substances occurs, allowing vasoconstrictor and proliferative effects to predominate (Figure 4) (Simsek et al. 2010; Xu and Zou 2009). It generally refers to an impaired maximal dilative response and/or an impaired sensitivity to endothelium dependent vasodilators such as acetylcholine, bradykinin and calcium ionophore, under conditions of preserved response to endothelium-independent dilators including sodium nitroprusside (Vanhoutte 2006).

Therefore, endothelial dysfunction is considered an early and independent predictor of poor prognosis in most forms of CVDs (Schächinger, Britten, and Zeiher 2000; Widlansky et al. 2003), with alterations in endothelial function consistently found in hypertension, atherosclerosis, T2DM and obesity (Vanhoutte 2006; Xu and Zou 2009). It is characterized by impaired endothelium-dependent vasodilation and endothelial activation, which is associated with a proinflammatory, proliferative and procoagulatory milieu that promotes initiation and complications of atherogenesis.

Endothelial dysfunction associated with insulin resistance appears to precede the development of overt hyperglycaemia in patients with T2DM, becoming a critical early target for the prevention of atherosclerosis and CVD in patients with diabetes mellitus or insulin resistance. A synergistic cross-talk exists between the conventional cardiovascular risk factors associated with diabetes mellitus contributing to disruption of endothelial integrity and acceleration of atherosclerosis.

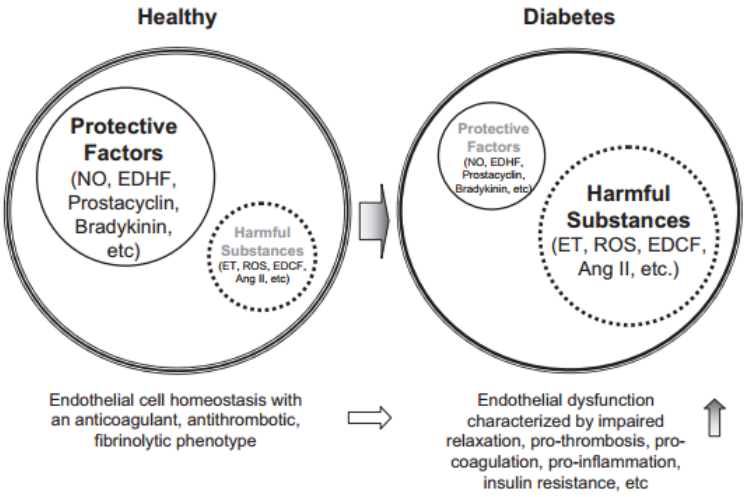

Figure 4: The crucial role of endothelium in the maintenance of vascular homeostasis. Maintenance of vascular homeostasis by the endothelium is accomplished through the release of vasoprotective factors and harmful. Damage to endothelium will disrupt the balance between them, initiating a number of events that promotes atherosclerosis (Xu and Zou 2009).

3.3. Hyperglycaemia as leading cause of endothelial dysfunction in diabetes

The physiopathology of endothelial dysfunction in diabetes mellitus has been extensively studied (Brownlee 2001; Xu and Zou 2009). Prolonged exposure to hyperglycaemia and insulin resistance are now recognized as the major factors implicated in the pathogenesis of diabetic specific microvascular and macrovascular complications (Xu and Zou 2009).

About hyperglycaemia, large prospective clinical studies show a strong relationship between glycaemia and cardiovascular complications in both T1DM and T2DM, as well as the large number of intracellular alterations that occurs in vascular tissue in the condition of high glucose levels (Brownlee 2001).

Early in the course of diabetes, intracellular hyperglycaemia causes abnormalities in blood flow and increased vascular permeability. This reflects decreased activity of vasodilators, increased activity of vasoconstrictors and augmented permeability to some factors such as vascular endothelial growth factor (VEGF). Quantitative and qualitative abnormalities of extracellular matrix contribute to an irreversible increase in vascular permeability. Long term a loss in microvascular cell occurs, partly due to a programmed cell death, and there is a progressive capillary occlusion as a result of both (i) extracellular matrix overproduction induced by growth factors such as the transforming growth factor-β (TGF-β); and (ii) periodically deposition of extravasated acid-Schiff-positive plasma proteins. Hyperglycaemia may also decrease production of trophic factors for endothelial and neuronal cells. Together, these changes lead to edema, ischemia and hypoxia-induced neovascularization in the retina, proteinuria, mesangial matrix expansion and glomerulosclerosis in the kidney and multifocal axonal degeneration in peripheral nerves.

3.3.1. Mechanisms of hyperglycaemia-induced endothelial damage

Animal and human studies have identified at least four major mechanisms to explain how hyperglycaemia causes diabetic cardiovascular complications (Brownlee 2001), and these are:

(i) Increased polyol pathway flux: aldose reductase is the first enzyme in the polyol pathway that reduces glucose to sorbitol, using NAD(P)H as a cofactor. In cells where aldose reductase activity is sufficient to deplete reduced glutathione (GSH), oxidative stress is augmented. Sorbitol dehydrogenase (SDH) oxidizes sorbitol to fructose using NAD^+ as a cofactor.

(ii) Increased advanced glycation end-products (AGEs) formation: AGEs are substances that derive from glycosylation reaction, which refer to the addition of a carbohydrate to a protein or lipid without the involvement of an enzyme. This non-enzymatic glycosylation of proteins and lipids interferes with normal protein function by disrupting molecular conformation, altering enzymatic activity, reducing degradation capacity and interfering with receptor recognition. In addition, glycosylated proteins interact with a specific receptor present on the cells which are relevant for the atherosclerotic process, including monocyte-derived macrophages, endothelial cells and smooth muscle cells. The interaction of glycosylated proteins with their receptor induces oxidative stress and proinflammatory cellular profile.

(iii) Activation of protein kinase C (PKC) isoforms: the PKC family comprises at least eleven isoforms, nine of which are activated by the lipid second messenger diacylglyceride (DAG). Hyperglycaemia increases the amount of DAG and this results in the activation of PKC in cultured microvascular cells (Koya and King 1998), as well as *in vivo* in the retina and renal glomeruli of diabetic animals (Pu Xia et al. 1994). Activation of PKC has a number of

pathogenic vascular consequences that contribute to hyperglycaemia induced-endothelial dysfunction. This mechanism has been largely explained in the paragraph 5 of this Section.

(iv) Increased hexosamine pathway flux: in order to decrease the excess of intracellular glucose, a part of it converts to the hexosamine pathway and it results in an increase of fructose-6-phosphate that is diverted from glycolysis to provide substrates for reactions that require UDP-N-acetylglucosamine, such as proteoglycan synthesis and the formation of O-linked glycoproteins. Inhibition of the rate-limiting enzyme in the conversion of glucose to glucosamine-6-phosphate through glutamine fructose-6-phosphate amidotransferase (GFAT), blocks hyperglycaemia-induced increase in the transcription of TGF-α, TGF-β1 and PAI-1. This leads to O-linked of various enzymes, above all transcription factors, and perturbs normal enzyme function. In addition to transcription factors, many other nuclear and cytoplasmic proteins are dynamically modified by O-linked glycosylation; an example relevant to diabetic complications is the inhibition of the endothelial nitric oxide synthase (eNOS) activity, which plays a critical role in developing cardiovascular complications in diabetes.

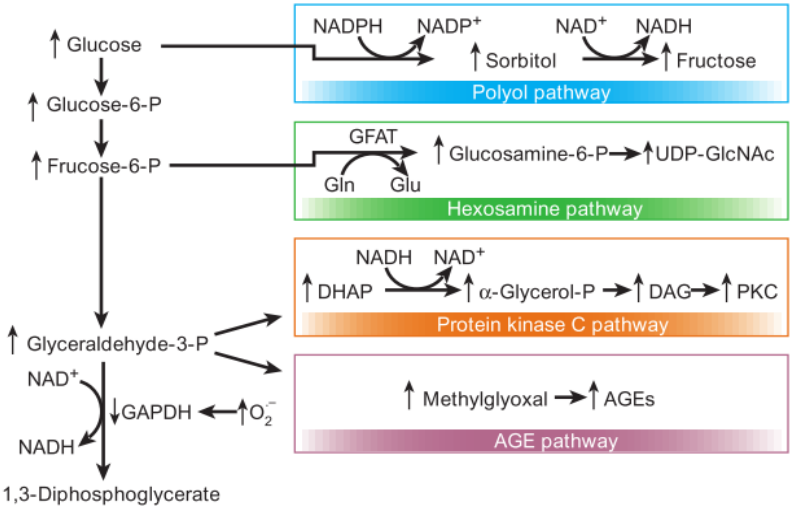

Figure 5: Mechanisms of hyperglycaemia-induced superoxide production. Excess superoxide partially inhibits GAPDH, thereby diverting upstream metabolites from glycolysis into pathways of glucose overutilization. This results in increased flux of DHAP to DAG, and of triose phosphates to methylglyoxal, the main intracellular AGE precursor. Increased flux of fructose-6-phosphate to UDP-N-acetylglucosamine increases modification of proteins by GlcNAc and increased glucose flux through the polyol pathway consumes NAD(P)H and depletes GSH (Brownlee 2001).

Each of the four different pathogenic mechanisms reflects a single process: the overproduction of superoxide ($\cdot O_2^-$), one of the majors reactive oxygen species, by the mitochondrial electron-transport chain (Brownlee 2001). According to this, ROS can be identified as the common denominator of hyperglycaemia-induced endothelial damage mechanisms, so oxidative stress that derives from ROS overproduction plays a central role in vascular physiology and pathophysiology (Griendling and FitzGerald 2003).

4. Incretins and cardiovascular disease

With the development of insulin radioimmunoassays for the study of glucose tolerance, a series of studies demonstrated that plasma levels of insulin were significantly greater after oral administration of glucose respect to the levels achieved following intravenous glucose challenge in normal human subjects (Drucker 2006). This gut-associated potentiation of insulin secretion was attributable to some neural factors, termed "incretins", and the capacity to potentiate insulin secretion following enteral nutrient ingestion is nowadays known as the "incretin effect" (Elrick 1964; Ussher and Drucker 2012).

The identity of the putative incretin factors remained unknown until 1970s, when glucose-dependent insulinotropic polypeptide (GIP) was purified and characterized (Cataland et al. 1974; Drucker et al. 1987). Although GIP was shown to be a potent stimulator of glucose-dependent insulin secretion, removal of GIP from gut extracts via immunoabsorption did not eliminate the incretin effect, providing evidence for the existence of additional peptides with incretin-like activity (Ebert, Unger, and Creutzfeldt 1983). The discovery of a second incretin hormone, glucagon-like peptide 1 (GLP-1), followed the cloning and sequencing of mammalian proglucagon gene. It encodes 2 peptides that were approximately 50% homologous to glucagon and for this reason they were named glucagon-like peptide-1 and glucagon-like peptide-2, as reviewed in Baggio & Drucker, 2007 (Baggio and Drucker 2007). Based on their homology to glucagon, both peptides were tested for insulinotropic activity, but they observed that only GLP-1 was capable of stimulating insulin secretion.

To date, only GIP and GLP-1 fulfill the definition of an incretin hormone in humans that promote glucose-dependent insulin secretion after meal ingestion (Drucker 2006). More studies have shown that these peptides potentiate glucose stimulated insulin secretion in an additive manner, likely contribute equally to the incretin effect, and together can fully account for the incretin effect in humans (Baggio and Drucker 2007).

4.1. GLP-1 and GLP-1 Receptor

GLP-1 is a 37 amino acid tissue-specific peptide produced from proglucagon in enteroendocrine L cells in response to nutrient ingestion, together with glicentrin, oxyntomodulin intervening peptide-2 and GLP-2 (Drucker 2006) (Figure 6).

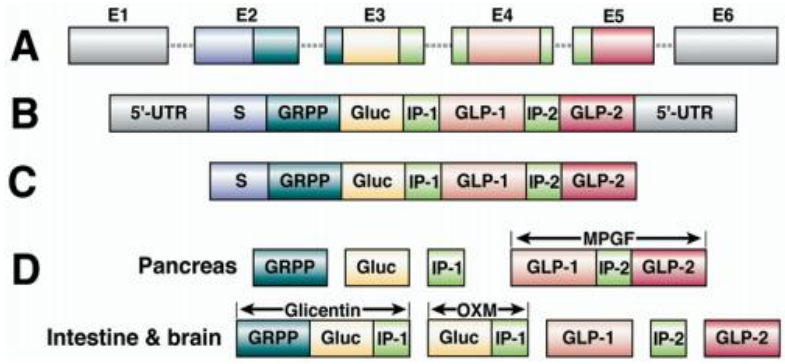

Figure 6: Structures of (A) the proglucagon gene, (B) mRNA, (C) protein, and (D) post-translational processing. In the pancreas proglucagon leads to the generation of glicentin-related polypeptide (GRPP), glucagon (GLUC), intervening peptide-1 (IP-1), and major proglucagon fragment (MPGF), whereas glicentin, oxyntomodulin (OXM), intervening peptide-2 (IP-2), and GLP-1 and GLP-2 are liberated in intestine and brain (Baggio and Drucker 2007).

GLP-1 stimulates insulin and inhibits glucagon secretion in a glucose-dependent manner. L cells are distributed throughout the small and large intestine; however, the majority of intestinal GLP-1 content has been localized to the distal small bowel and colon. GLP-1 is also produced in the central nervous system (CNS), predominantly in the brainstem, and subsequently transported to a large number of regions within the CNS.

GLP-1 exerts its actions on multiple organs and tissues, in order to lower blood glucose levels and to improve glucose control in T2DM patients (Drucker 2007). A part from its role on pancreatic β-cells stimulating insulin production and on α-cells inhibiting glucagon secretion, GLP-1 acts directly on heart, stomach, brain and kidney, whereas its effects on liver, muscle and adipose tissue are indirect (Baggio and Drucker 2007; Ban et al. 2008; Drucker 2003) (Figure 7).

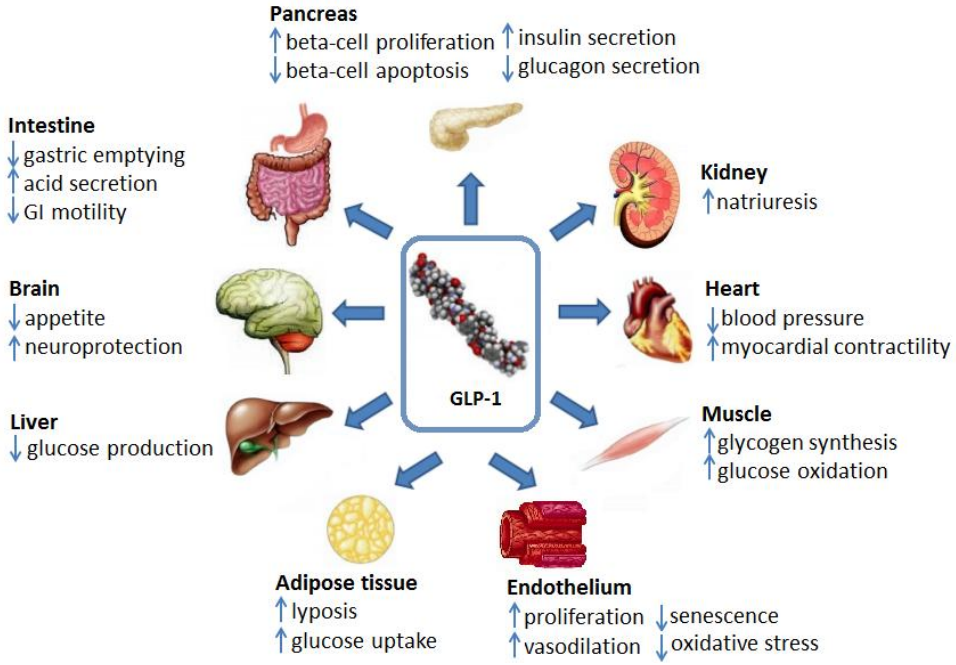

Figure 7: The multiple actions of GLP-1 to improve glucose control in T2DM. GLP-1 acts directly or indirectly on several peripheral tissues that contribute to lower blood glucose levels. Adapted from Ussher et al. (Ussher and Drucker 2012).

As GLP-1 has a short half-life due to its rapid degradation mediated by the enzyme dipeptidyl dipeptidase-4 (DPP-4), therapeutic strategies for patients with T2DM are focused in increasing the presence of GLP-1 in blood circulation, either by inhibiting DPP-4 activity (e.g. sitagliptin, vildagliptin, linagliptin, saxagliptin, alogliptin) or by using degradation-resistant GLP-1 analogues (e.g. exenatide, liraglutide, albiglutide, lixisenatide).

GLP-1 functions through its own specific receptor, GLP-1 receptor (GLP-1R). Human GLP-1R is a 463 amino acid heptahelical G protein-coupled receptor (GPCR) (Drucker 2006). It transduces the majority of GLP-1 actions *in vivo* and, although numerous studies allege the functional existence of a second GLP-1 receptor, only a single GLP-1R coupled to glucose homeostasis has yet been identified (Drucker 2006; Thorens et al. 1993). The GLP-1R was originally identified in islet β-cells but it is widely expressed in extrapancreatic tissues, including the lung, kidney, central nervous system, enteric and peripheral nervous system, lymphocytes, blood vessels and heart (Bullock, Heller, and Habener 1996; Thorens et al. 1993).

The N-terminal extracellular region of the GLP-1R is essential for GLP-1 binding, whereas distinct domains within the third intracellular loop are critical for efficient coupling of the receptor to specific G-proteins (Baggio and Drucker 2007).

The GLP-1R can couple different G proteins (Gαs, Gαq, Gαi, and Gαo) (Montrose-Rafizadeh et al. 1999) leading to increases in intracellular Ca^{2+}, adenylate cyclase (AC) and phospholipase C (PLC), and activation of protein kinase A (PKA), protein kinase C (PKC), phosphoinositide 3-kinase (PI3K) and mitogen-activated protein kinase (MAPK) signal transduction pathways (Montrose-Rafizadeh et al. 1999; Thorens et al. 1993).

As it has been described for all GPCRs (Drake, Shenoy, and Lefkowitz 2006), also GLP-1R undergoes to a specific trafficking in the cell. Briefly, GLP-1R initially resides in the ER, where it is processed and opportunely folded by chaperones and quality-control proteins. Following ER exit, GLP-1R transits through the Golgi apparatus, and here, in the distal edge, it is packaged in exocytic transport vesicles and enters the endosomal system, where it is subsequently targeted to the plasma membrane. Multiple proteins have been identified that affect GLP-1R stability at the cell surface: although variations have been described, GLP-1R endocytosis from the plasma membrane most commonly occurs in a G protein-coupled receptor kinase (GRK)- and β-arrestin - dependent manner (Shenoy et al. 2006). Ligand binding promotes GRK mediated phosphorylation of the cytoplasmic surface of the GLP-1R and subsequent β-arrestin translocation and binding to the receptor. β-arrestin binding, in turn, facilitates the subsequent recruitment of AP-2 and clathrin and this leads to the GLP-1R inclusion in clathrin-coated pits (CCPs) before endocytosis via clathrin-coated vesicles (CCVs). C, Following endocytosis, GLP1-R may be either recycled to the plasma membrane or sorted for lysosomal degradation (Drake, Shenoy, and Lefkowitz 2006).

4.2. Pancreatic effects of GLP-1 signalling

GLP-1 produces several biological actions in the pancreas (Figure 17). GLP-1 directly potentiates and regulates β-cell insulin secretion, minimizing the risk of hypoglycemia in diabetic subjects; also induces glucose competence in previously unresponsive α-cells (Holz, Kühtreiber, and Habener 1993) and rapidly improves β-cell glucose sensitivity, thereby restoring insulin secretion toward normal levels in human patients with T2DM (Rachman et al. 1996).

The binding of GLP-1 to its specific receptor on pancreatic β-cells leads to activation of adenylate cyclase activity and production of cAMP. cAMP mediates its stimulatory effect on insulin secretion via 2 distinct mechanisms (Baggio and Drucker 2007): (1) PKA-dependent phosphorylation of downstream targets and (2) PKA-independent activation of the exchange factor directly activated by cAMP (EPAC), that is involved in other important functions (Figure 8).

GLP-1 also stimulates β-cell proliferation and neogenesis and inhibits β-cell apoptosis, thereby increasing β-cell mass (Buteau et al. 2003) The proliferative effects of GLP-1R agonists are mediated via transactivation of the epidermal growth factor receptor (EGRP), which leads to increases in PI3K and activation of PKCζ (Buteau et al. 2003) and/or Akt/PKB. GLP-1 also stimulates β-cell replication via IRS-2 signalling (S. Park et al. 2006), as well as activation of cAMP/PKA, PI3K, and MAPK signalling pathways, and up-regulation of expression of the cell cycle regulator cyclin D1 (Baggio and Drucker 2007). The specific mechanisms involved in GLP-1-dependent β-cell differentiation/neogenesis are not well defined but likely involve activation of PKC and MAPK, as well as synergistic interaction with TGFβ and regulation of SMAD transcription factor activity. The transcription factor FoxO1, a key negative regulator of β-cell growth, also plays an important role in mediating the proliferative and cytoprotective effects of GLP-1 on the β-cell (Baggio and Drucker 2007). The molecular mechanisms that couple GLP-1R activation to β-cell mass expansion and cytoprotection also include the activation of the transcription factor Pdx-1 (Wang et al. 1999), which appears to be a shared component in all

GLP-1R- dependent molecular pathways. Finally GLP-1 improves β-cell endoplasmic reticulum stress enhancing ATF4 translation, GADD34 expression and eIF2α dephosphorylation (Baggio and Drucker 2007), as detailed in the paragraph 9 of this section.

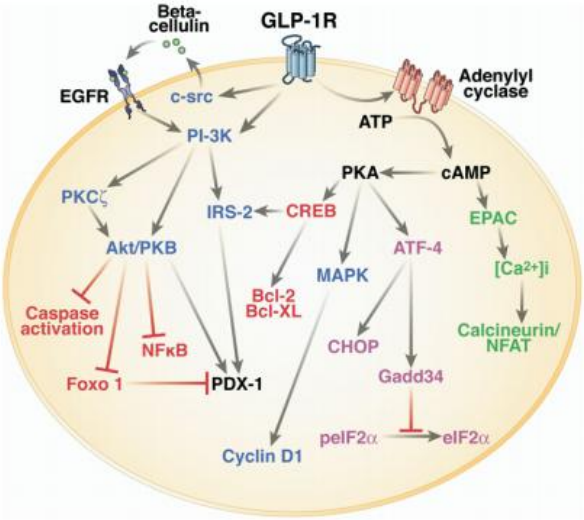

Figure 8: GLP-1 signalling in pancreatic β-cells. In pancreatic β-cells binding of GLP-1 to its receptor results into the activation of various intracellular signal transduction pathways that ensure insulin secretion and biosynthesis (green), proliferation and neogenesis (blue), inhibition of apoptosis (red), and ER stress reduction (purple) (Baggio and Drucker 2007).

4.3. Vascular effects of GLP-1 signalling

GLP-1R has been detected in human coronary artery endothelial cells (HCAECs) and human umbilical vein endothelial cells (HUVECs) (Ding and Zhang 2012; Y. Ishibashi et al. 2011; Nyström et al. 2004; Oeseburg et al. 2010) as well as in mouse coronary endothelial and smooth muscle cells (Ban et al. 2008). As shown in Figure 9, the first consequence of GLP-1 binding to its endothelial receptor is the activation of cAMP, that in turn activates PKA (Ussher and Drucker 2012). The involvement of cAMP/PKA-dependent and independent pathways to decrease apoptosis by inhibiting caspase activation has been demonstrated in endothelial cells (Saraiva and Sposito 2014).

The main mechanisms of cardioprotective effects of GLP-1 have been studied in HAECs. GLP-1 analogue exendin-4 stimulates proliferation of HAECs *in vitro* and this effect is mediated through PKA- and PI3K/AKT/eNOS-activation pathways via a GLP-1 receptor-dependent mechanism (Erdogdu et al. 2010). It has been demonstrated that AKT, a factor downstream of PI3K, participates in insulin signalling pathways and regulates many cellular events, including cell proliferation (Montagnani et al. 2002; Muniyappa et al. 2007) and responds to the cellular actions of both GLP-1 or exendin-4 in different cellular tissues like pancreas or liver (Hui et al. 2003; Redondo et al. 2003). Also for HCAECs, stimulation with exendin-4 leads to the activation of AKT (Erdogdu et al. 2010).

Apart from its role in linking the GLP-1 signal to the intracellular machinery that modulates cell proliferation (Q. Wang et al. 2004), AKT is also responsible of the phosphorylation of eNOS (Muniyappa and Sowers 2013; Muniyappa et al. 2007), the crucial factor in regulating redox homeostasis in endothelial cells (Nyström et al. 2004). Erdogdu et al. demonstrated that stimulation of the HCAECs with exendin-4 induces activation of both Akt and eNOS (Erdogdu et al. 2010). Inhibition of AKT by a specific inhibitor for PI3K or AKT abolishes the activation of eNOS and cell proliferation stimulated by exendin-4.

In endothelial cells, activation of PI3K/AKT can be achieved by PKA and this signalling is involved in both cell proliferation and apoptosis (Torella et al. 2009). A direct interaction of PKA with AKT in endothelial cells has been also reported (Bellis et al. 2009). So, as described for pancreas, there is a considerable overlap between pathways induced by the GLP-1R activation also in endothelium

(Saraiva and Sposito 2014). Erdogdu et al. demonstated that in HAECs response to exendin-4 is completely blocked by inhibition of PKA, suggesting a crucial role of PKA in these events (Erdogdu et al. 2010).

The positive actions of GLP-1 and its analogues on endothelium have been studied also in HUVEC cells. In HUVECs cultured during 24h, treatment with GLP-1 has no effect on AKT phosphorylation but increases PKA activity and cAMP response element-binding protein (CREB) phosphorylation (Oeseburg et al. 2010), demonstrating that HUVECs are a direct target for GLP-1 action.

Direct treatment of HUVEC cells with the GLP-1 analogue liraglutide increases eNOS phosphorylation and NO production via AMPK (Hattori et al. 2010). Furthermore, treatment with GLP-1 reduces ROS and VCAM-1 gene expression in HUVECs after exposure to AGEs (Ishibashi et al. 2010). Liraglutide also prevents the increase in PAI-1 and VCAM-1 mRNA and protein expression in response to TNFα or hyperglycaemia in HUVEC cells (Liu et al. 2009). Using an *in vitro* model of vascular aging, treatment of HUVECs with GLP-1 or exendin-4 reduces the number of senescent cells in an exendin(9 –39)-sensitive manner (Oeseburg et al. 2010b). These effects are also dependent on PKA activity because they are abolished by pretreatment with of its chemical inhibitors of PKA H89 (Oeseburg et al. 2010).

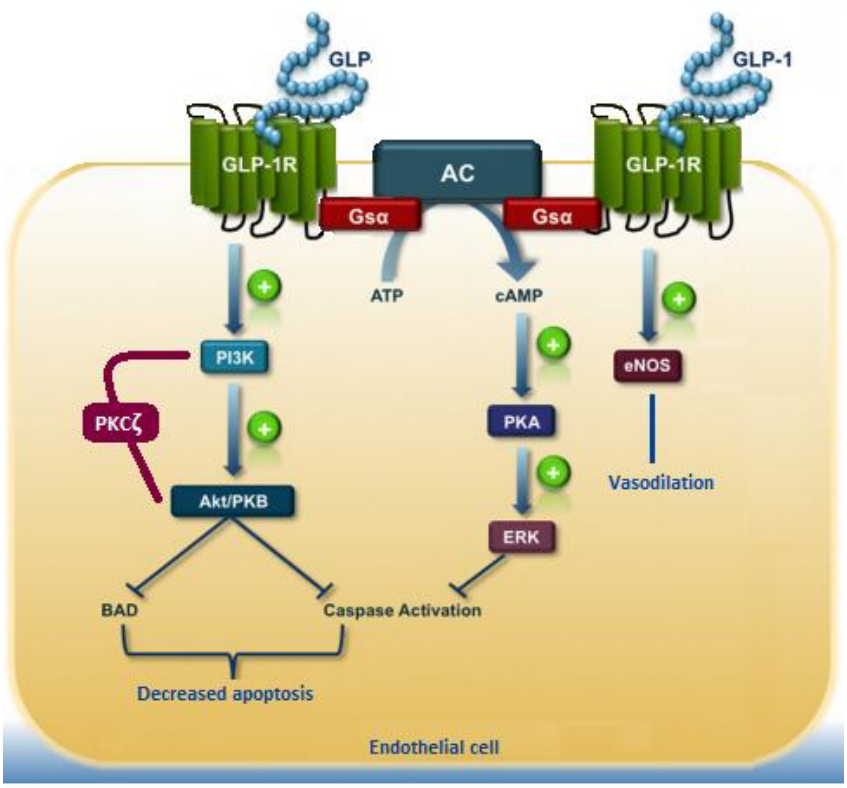

Figure 9: GLP-1R signal transduction pathways in the endothelial cell. The signalling pathway downstream of the GLP-1R involves the cAMP that in turn activates PKA and ERK, decreasing apoptosis by inhibiting caspase activation. The anti-apoptotic properties of GLP-1 are also mediated by the PI3K/PKCζ/AKT via inhibition of caspase and BAD expression. Activation of PI3K/AKT can be achieved by PKA and this signalling is involved in both cell proliferation and apoptosis. GLP-1R signal transduction is finally involved in eNOS phosphorylation and NO production. Adapted from Ussher et al. (Ussher and Drucker 2012).

4.4. GIP and GIP Receptor

GIP is a 42 amino acid peptide synthesized in and secreted from enteroendocrine K cells localized to the proximal small bowel (Ussher and Drucker 2012b). Like GLP-1, GIP is secreted at low basal levels in the fasted state and plasma levels of GIP increase within minutes of nutrient ingestion. Although the major action of GIP is the glucose-dependent stimulation of insulin secretion, GIP also promotes lipid uptake and expansion of adipocyte mass and exerts a number of extrapancreatic actions in the brain, bone, and adrenal gland, delineated predominantly in preclinical studies (Kulkarni 2010).

The GIP receptor (GIPR) is a member of the class B family of GPCR. Its activation leads to cAMP generation and insulin secretion from islet β-cells. The GIPR is widely expressed in extrapancreatic tissues, including the gastrointestinal tract, adipose tissue, heart, pituitary, adrenalcortex, and multiple regions of the CNS (Usdin et al. 1993). Disruption or attenuation of GIP action is associated with diminished weight gain, resistance to diet-induced obesity, and improved insulin sensitivity in preclinical studies (Irwin and Flatt 2009; Kulkarni 2010), whereas genetic variation within the human Gipr gene is linked to control of postprandial glucose and body weight (Saxena et al. 2010; Speliotes et al. 2010).

4.5. DPP-4 and incretin degradation

The half-life of bioactive GLP-1 in the circulation is less than 2 minutes, being rapid inactivated by the DPP-4 (Deacon et al. 1995). DPP-4 was originally described as a lymphocyte cell surface protein named cluster of differentiation 26 (CD26). It is a ubiquitous proteolytic enzyme that specifically cleaves dipeptides from the amino terminus of oligopeptides or proteins that contain an alanine or proline residue in position 2, modifying or inhibiting their activity. DPP-4 is ubiquitously expressed and can be found in multiple tissues and cell types including kidney, lung, adrenal gland, liver, intestine, spleen, testis, pancreas, and CNS, as well as on the surface of lymphocytes and macrophages (Ussher and Drucker 2012a). Notably, DPP-4 also has been found localized in smooth muscle and endothelial cells in different species (Matheeussen et al. 2011; Palmieri and Ward 1989).

GLP-1 is a substrate for DPP-4 and is metabolized rapidly to its inactive forms GLP-1 (9-37) or GLP-1 (9-36) amide (Ussher and Drucker 2012). DPP-4 inhibitors bind to DPP-4 to prevent the breakdown of GLP-1, thus increasing the half-life and bioavailability of active GLP-1, and in turn enhancing its physiological effects. The observation that DPP-4 cleaves GLP-1 at the N terminus (Deacon et al. 1995; Kieffer, McIntosh, and Pederson 1995; Mentlein, Gallwitz, and Schmidt 1993), followed by demonstrations that chemical inhibition or genetic inactivation of DPP-4 increases the circulating levels of intact GLP-1 (Holst and Deacon 1998; Marguet et al. 2000), established DPP-4 as a major regulator of incretin degradation.

It has been demonstrated that short-term exposure to high glucose induces DPP-4 activity in microvascular endothelial cells (Pala et al. 2012). Although the precise biological role of DPP-4 in the cardiomyocyte, endothelial or coronary smooth muscle cells requires further studies, DPP-4 is also a circulating protein and thus DPP-4 activity in the systemic and coronary circulation may influence intact levels of GLP-1 and other vasoactive DPP-4 substrates reaching the myocardium and vasculature.

4.6. Effects of GLP-1 agonists and DPP-4 inhibitors in endothelium

Elucidation of GLP-1 actions in the vascular system has important implications for the treatment of subjects with T2DM. Studies in animals and humans have explored the biological actions of GLP-1 on the myocardium and the vasculature, as well as on cardiovascular risk factors.

4.6.1. Direct effects on endothelial function *in vitro*

As described before, GLP-1 was shown to attenuate the TNF-α-mediated induction of PAI-1 expression (Liu et al. 2008) and to inhibit AGEs-induced up-regulation of VCAM-1 in HUVECs (Yuji Ishibashi et al. 2010). It also up-regulates the activity and protein expression of eNOS in HUVECs through GLP-1R -dependent and -independent pathways (Ding and Zhang 2012). GLP-1 prevents ROS-induced cell senescence through the activation of PKA in HUVECs (Oeseburg et al. 2010). It also decreases high glucose-induced ROS production and the apoptotic index, as well the levels of NAD(P)H oxidase and Rho-expression, with increases in the cAMP/PKA activity in cardiac microvascular endothelial cells (Wang et al. 2013).

Moreover, GLP-1 restores the oxidized LDL-induced loss of cell viability in accordance with a significant decrease in intracellular NO activity. It suppresses the lipid peroxidation, restores the activities of endogenous antioxidants and decreases the levels of NO and cell apoptosis by preventing the up-regulation of poly (ADP-ribose) polymerase-1/nitrotyrosine and inducible NO synthase protein in islet microvascular endothelial cells (Liu et al. 2011). GLP-1 also improves the proliferation and differentiation of endothelial progenitor cells (EPCs) by up-regulating VEGF (Xiao-Yun et al. 2011).

Exendin-4 stimulates proliferation of human coronary artery endothelial cells through eNOS-, PKA- and PI3K/Akt-dependent pathways via the GLP-1 receptor (Ö Erdogdu et al. 2010). Exendin-4 also restores the eNOS-induced ROS production in response to lipotoxicity and protects against lipoapoptosis through PKA-PI3K/Akt-eNOS-p38 MAPK-JNK-dependent pathways via a GLP-1 receptor dependent mechanism (Özlem Erdogdu et al. 2013).

Liraglutide prevents high glucose-induced endoplasmic reticulum stress in HUVECs (Schisano et al. 2012) and inhibits TNF-α-induced ICAM-1 and VCAM-1 expression, and these effects are dependent on the GLP-1R (Gaspari et al. 2011).

Moreover, it has been demonstrated that liraglutide attenuates TNF-α-induced ROS productionand that it increases the expression of anti-oxidant enzymes, including Superoxide Dismutase-1 (SOD1) and -2 (SOD2) in HUVECs (Shiraki et al. 2012).

As DPP-4 inhibitors that maintain the plasma levels of active GLP-1, it has been demonstrated that sitagliptin augments the protective effects of GLP-1 increasing eNOS mRNA levels in AGEs-exposed HUVECs (Ishibashi et al. 2011). Alogliptin induces vascular relaxation via NO and endothelial-derived hyperpolarizing factor-mediated mechanisms, and increases the NO production with increased eNOS phosphorylation in HUVECs (Shah et al. 2011). Since decreasing the oxidative stress results in a restoration of the eNOS function, all of these phenomena, including the decreased ROS production and increased eNOS expression, in addition to the endothelial repair and promotion of angiogenesis, lead to an amelioration of the endothelial function.

4.6.2. The *in vivo* or *ex vivo* endothelial function

Exendin-4 significantly increases NO levels, improving vasodilatation, and reduced the expression of NF-κB in the aortas isolated from obese rats. This has been demonstrated to occur through the cAMP or AMPK-eNOS pathways (Han et al. 2012). Exendin-4 also inhibits the formation of atherosclerotic lesions in apolipoprotein E deficient ($ApoE^{-/-}$) mice (Arakawa et al. 2010).

Liraglutide improves the endothelial function via GLP-1R, increases eNOSs level and reduces the ICAM-1 expression in the aortic endothelium in mice (Gaspari et al. 2011). Liraglutide also inhibits the progression of atherosclerotic plaques, and improves the plaque stability in $ApoE^{-/-}$ mice (Gaspari et al. 2013).

Sitagliptin protects the endothelial function of the renal artery in spontaneously hypertensive rats, and exenatide ameliorats the endothelial dysfunction in the renal arteries from hypertensive patients in an *ex vivo* study (Liu et al. 2012). On the other hand, Nathanson et al. reported that the endothelial dysfunction induced by triglycerides is not restored by exendin-4 treatment in rat conduit arteries *ex vivo* (Nathanson et al. 2009).

5. Protein Kinase C and its impact on diabetic complications

As explained before, multiple biochemical pathways have been proposed to link the adverse effects of hyperglycaemia with vascular complications. Cellular mechanisms include increased activation of the polyol pathway, increased AGEs production, increased hexosamine pathway flux and activation of the DAG-PKC pathway.

The DAG-PKC pathway is one of the most studied pathways in cellular signalling induced by diabetes (Nishizuka 1992).

5.1. Activation of DAG-PKC pathway in diabetes

Diacylglycerol functions as a second messenger signalling lipid and is a product of the hydrolysis of the phospholipid phosphatidylinositol 4,5-bisphosphate (PIP_2) that occurs after ligand activation of G-protein-coupled receptors. PIP_2 is hydrolyzed by the enzyme phospholipase C (PLC) (a membrane-bound enzyme) that, through the same reaction, together with DAG, also produces inositol trisphosphate (IP_3) (Rask-Madsen and King 2005). Although IP_3 diffuses into the cytosol, DAG remains within the plasma membrane, due to its hydrophobic properties. IP_3 stimulates the release of calcium ions from the smooth endoplasmic reticulum, whereas DAG is a physiological activator of PKC. The production of DAG in the membrane facilitates translocation of PKC from the cytosol to the plasma membrane.

DAG levels are chronically increased in vascular tissues such as retina (Shiba et al. 1993), aorta, heart and renal glomeruli (Ishii et al. 1996) of diabetic subjects, due to an increase in the glycolytic intermediate dihydroxyacetone phosphate. This intermediate is reduced to glycerol-3-phosphate, which subsequently increases *de novo* synthesis of DAG (Pu Xia et al. 1994).

In vitro different studies have shown that DAG levels increase in a time-dependent manner when glucose levels elevate from 5.5 to 22 mM in aortic endothelial cells (Inoguchi et al. 1992), retinal pericytes (Geraldes et al. 2009), smooth muscle cells (Pu Xia et al. 1994) and renal mesangial cells (Ayo et al. 1991).

PKC, a group of enzyme members of the AGC (cAMP-dependent protein kinase/protein kinase G/protein kinase C) family, is a serine/threonine-related protein kinase that plays a key role in many cellular functions and affects many signal transduction pathways (Rask-Madsen and King 2005). There are multiple isoforms of PKC that function in various biological systems (Steinberg 2008) (Figure 10):

- conventional PKC (cPKC) isoforms (PKC-α, -β1, -β2, -γ) are activated by DAG, phosphatidylserine (PS), calcium and phorbol 12-myristate 13-acetate (PMA);
- novel PKCs (nPKC; PKC-δ, -ε, -θ and -η) are activated by DAG, PS or PMA, but not by calcium;
- atypical PKCs (aPKC; PKC-ζ and -ι/λ) are not activated by calcium, DAG or PMA.

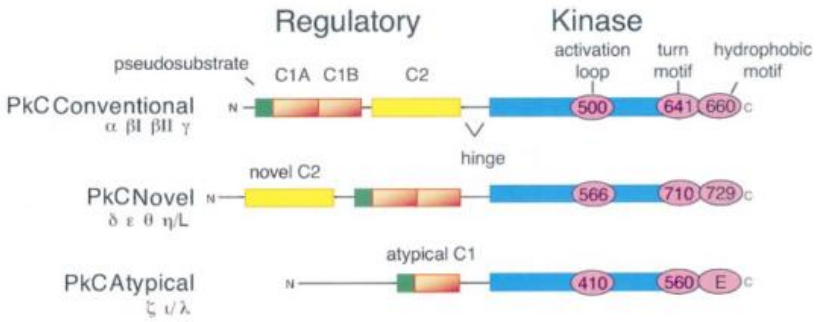

Figure 10: Primary structure of the PKC isoforms. All isoenzymes have a conserved kinase core (cyan) and C-terminal extension that contains three conserved phosphorylation sites (pink). The C1 domain (orange) functions as a DAG/PMA sensor. C2 domain (yellow) of conventional PKCs serves as a Ca^{2+}-sensor (Newton 2003).

PKCs can also be activated by oxidants such as H_2O_2 (Konishi et al. 1997) or by mitochondrial superoxide produced following high glucose levels (Nishikawa et al. 2000).

The structure of all PKCs consists of a regulatory domain and a catalytic domain linked by a hinge region (Figure 10).

The regulatory domain is at the N-teminus of the PKCs and contains several shared subregions. The C1 domain, present in all of the isoforms of PKCs, has a binding site for DAG and the phorbol ester PMA. This domain is functional and capable of binding DAG in both conventional and novel isoforms, but not in atypical PKCs. The C2 domain acts as a Ca^{2+} sensor and is present in both conventional and novel isoforms, but functional as a Ca^{2+} sensor only in the conventional. The pseudosubstrate region, which is present in all three classes of PKCs, is a small sequence of amino acids that binds the substrate-binding cavity in the catalytic domain, keeping the enzyme inactive. When Ca^{2+} and DAG are present in sufficient concentrations, they bind to the C2 and C1 domain, respectively, and recruit PKC to the membrane. This interaction with the membrane results in release of the pseudosubstrate from the catalytic site and activation of the enzyme.

The catalytic region or kinase core has a bilobal structure with a β-sheet comprising the N-terminal lobe and an α-helix constituting the C-terminal lobe. Both the ATP- and substrate-binding sites are located in the cleft formed by these two lobes. This is also where the pseudosubstrate domain of the regulatory region binds. An essential feature of the catalytic region for PKC activation is its phosphorylation. The conventional and novel PKCs have three phosphorylation sites, the activation loop, the turn motif, and the hydrophobic motif. The atypical PKCs are phosphorylated only on the activation loop and the turn motif. 3-phosphoinositide-dependent protein kinase-1 (PDK1) is the upstream kinase responsible for initiating the process by transphosphorylation of the activation loop.

Upon activation, PKC is translocated to the plasma membrane by RACK proteins (membrane-bound receptor for activated PKC proteins). There it remains activated after the original activation signal or the Ca^{2+}-wave is gone.

Many abnormal vascular processes, including endothelial dysfunction, vascular permeability, angiogenesis, cell growth and apoptosis, alterations in crucial enzymes and transcriptional factors are attributed to multiple PKC isoforms that are modified in hyperglycaemia and diabetes (Newton 2003) (Figure 11).

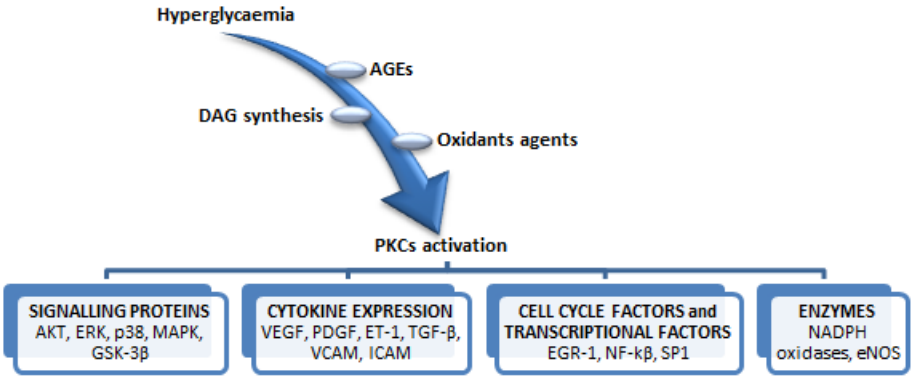

Figure 11. Biological targets of PKCs isoforms. In diabetes mellitus, hyperglycaemia is responsible of elevated DAG production, a physiological activator of the different forms of PKCs. Once produced, PKCs in turn activate diverse signalling pathways mediated by AKT, ERK, p38 and MAPK; also they induce the expression of inflammatory, cell cycle related and transcription factor. Finally they are involved in the enhancement of some enzymes responsible of ROS production, such as NAD(P)H oxidases and eNOS (Geraldes and King 2010)

5.2. PCK activation in endothelium

As explained before, ECs play a crucial role in regulating both vasodilator and vasoconstrictor substances mediating coagulation, platelet adhesion and immune function. Also they are involved in the control of volume and electrolyte content of the intravascular and extravascular spaces (Geraldes and King 2010).

Tight junctions between ECs form a vascular barrier, which in a condition of elevated glucose levels, undergoes to abnormalities and becomes more vulnerable and permeable (Geraldes and King 2010). An explication of these changes in tight junctions is reconnected to activation of the DAG-PKC pathway, which directly increases the permeability of albumin and other macromolecules (Lynch et al. 1990; Wolf et al. 1991).

Inoguchi and collaborators reported that hyperglycaemia inhibits gap junction intercellular communication in bovine aortic ECs (Inoguchi et al. 1995). Staurosporine, a serine/threonine kinase inhibitor, prevented these effects generated by high glucose and PKC activation (Inoguchi et al. 1995). Moreover, it has been shown that high glucose exposure induced translocation of PKC-α, -β1, -β2, and PKC-δ but not PKC-ε or PKC-ζ in retinal ECs (Park et al. 2000). A previous study showed that overexpression of PKC-β1 in human dermal microvascular ECs enhanceed phorbol ester-induced increased permeability to albumin (Nagpala et al. 1996). Hempel and colleagues also showed that PMA increased permeability via translocation of PKC-α similar to that caused by high glucose levels and that this permeability was prevented by staurosporine (Hempel et al. 1997).

PKC activation is responsible not only of abnormalities in tight junctions, but also of endothelial dysfunction, being involved in alterations of NO bioavailability and VEGF expression as well as in decreased production of prostacyclin and increased thromboxane and ET-1 (Cardillo et al. 2002; Cosentino et al. 2003; Hink et al. 2001).

A previous study demonstrated that eNOS expression is decreased in aortic ECs cultured in high glucose concentrations, resulting in a reduction of NO (Y. Ding et al. 2000). Treatment with calphostin C, an inhibitor of c- and nPKC, prevented reduction in NO production caused by high glucose

(Cosentino et al. 2003). Apart from the enzyme eNOS, another potential pathway by which high concentrations of glucose modulate NO bioavailability is by increasing superoxide production from NAD(P)H oxidase in aortic ECs (Inoguchi et al. 2000). The induction of several subunits of NAD(P)H oxidase by constant or intermittent high glucose concentrations is decreased when PKC-β activation is inhibited (Quagliaro et al. 2003).

PKC activation also modulates vascular endothelial permeability and neovascularization via the expression of growth factors, such as VEGF. It has been shown that mitogenic and permeability actions of VEGF are, in part, the result of the membrane expression of PKC-α and -β through tyrosine phosphorylation of phospholipase-Cγ, which is reduced when PKC-β is specifically inhibited (Pu Xia et al. 1996).

5.3. PKC Inhibitors and human clinical trials

Non-specific PKCs isoform inhibitors have been developed, but they can interact with other ATP binding kinases resulting in toxic and severe side effects *in vivo*. Suitable specific PKCs isoform inhibitors for therapeutic or clinical studies should target the regulatory domain or bind to the substrate or ATP binding site of the catalytic domain (Geraldes and King 2010).

The most studied PKC inhibitor in cellular, animal and especially human studies (Geraldes and King 2010) is Ruboxistaurin (LY333531, RBX or Arxxant™; Eli Lilly and Company, Indianapolis, IN), a class of bisindoylmaleimide (Ishii et al. 1996; Koya et al. 2000) that shows selective inhibition for PKC-β1 and PKC-β2 (Jirousek et al. 1996).

Phase I studys using RBX included patients who had diabetes for less than 10 years and no evidence of clinical retinopathy (Aiello et al. 2006). This study determined the dose needed to normalize the retinal blood flow (RBF), an early marker of diabetic retinopathy. The dose-response curve showed that a minimum dosage of 32 mg/day orally is required to prevent decreases in RBF in diabetic patients (Aiello et al. 2006). Few side effects were found during clinical trials of up to four years' duration (McGill et al. 2006). Phase II and phase III clinical trials were conducted in late stages of non-proliferative diabetic retinopathy, with the loss of visual acuity as the primary end point.

The first two clinical trials, *PKC-Diabetic Retinopathy Study* (PKC-DRS) and *PKC Diabetic Macular Edema Study* (PKC-DMES) (Milton and Sheetz 2008), failed to reach primary outcomes due to multiple factors (unpowered, three treatment arms of differing dosages, high drop-out rate of patients). However, the *PKC-Diabetic Retinopathy Study 2* (PKC-DRS2) (PKC-DRS2 Group et al. 2006) showed that RBX significantly prevents reduction of visual acuity in diabetic patients with moderate visual loss and decreases the onset of diabetic macular edema. These clinical results suggest that PKC activation, especially of the -β isoform, participates in the development of diabetic retinopathy. However, because treatment with RBX preserves visual acuity by decreasing capillary permeability or targeting the neural retina but cannot significantly delay the progression of diabetic retinopathy (PKC-DRS2 Group et al. 2006), these data suggest that inhibition of the PKC-β isoform alone is not enough to stop the early metabolic changes that occur in diabetic retinopathy (Geraldes and King 2010).

The role of PKC-β was also evaluated in T2DM patients with nephropathy. In kidney biopsies of diabetic subjects, there was an increase of PKC-β mRNA expression as compared to control subjects (Langham et al. 2008). A phase II clinical trial was conducted using RBX (32 mg/day) to determine whether PKC-β inhibition can be effective in these patients and results suggested that one year of treatment is able to decrease the loss of glomerular filtration rate and proteinuria (Tuttle et al. 2005).

Abnormal endothelial function induced by hyperglicaemia has been demonstrated in T2DM as well as in T1DM and obese subjects (Calver, Collier, and Vallance 1992; McVeigh et al. 1992; Steinberg et al. 1996). A preliminary study showed that the vascular permeability is increased as early as 4–6 weeks' duration of diabetes in patients, supporting the concept of endothelial dysfunction (Williamson et al. 1987). Treatment with RBX prevented endothelium-dependent vasodilatation abnormalities induced by hyperglycaemia (Beckman et al. 2002). Moreover, a recent study in T2DM subjects showed that 6 weeks treatment of RBX improves femoral-mediated dilatation at 1 and 5 minutes after cuff deflation as compared to placebo (Mehta et al. 2009). These data suggest that PKC activation, especially the -β isoform induced by hyperglycaemia, may be responsible for the endothelial dysfunction.

Although these results are very encouraging, further studies are needed to determine whether RBX can effectively improve endothelial function in T2DM.

6. Reactive oxygen species, antioxidant response and oxidative stress

All layers of the vascular wall have enzymatic systems capable of producing reactive oxygen species. ROS is a collective term encompassing both oxygen radicals and certain non-radicals which act as oxidizing agents and/or are easily converted into radicals. ROS include: superoxide anion (O_{2^-}), hydroxyl radical (OH^-), nitric oxide (NO), lipid radicals (LOO^-), hydrogen peroxide (H_2O_2), hypochlorous acid (HOCl) and peroxynitrite ($ONOO^-$) (Hua Cai and Harrison 2000) (Figure 12). Principal among these is O_2, formed from the univalent reduction of oxygen: its unpaired electron renders it highly reactive and unstable with a short half-life. Superoxide acts as both an oxidizing agent, being reduced to H_2O_2, and a reducing agent, donating its extra electron to form $ONOO^-$ with NO (Darley-Usmar, Wiseman, and Halliwell 1995).

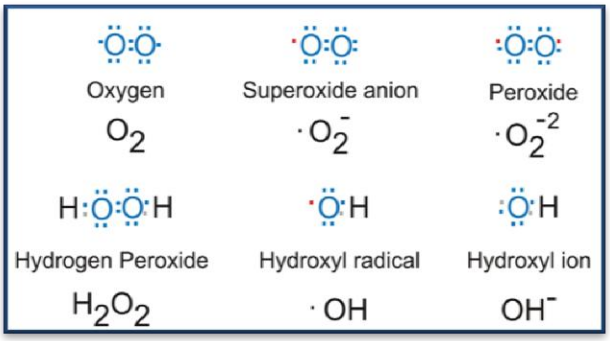

Figure 12: Electron structures of common reactive oxygen species. Most ROS are generated as by-products during mitochondrial electron transport. In addition ROS are formed as necessary intermediates of metal catalyzed oxidation reactions. Atomic oxygen has two unpaired electrons in separate orbits in its outer electron shell. This electron structure makes oxygen susceptible to radical formation. The sequential reduction of oxygen through the addition of electrons leads to the formation of a number of ROS including: superoxide; hydrogen peroxide; hydroxyl radical and hydroxyl ion.

These molecules are principally derived from the oxygen that is consumed in various metabolic reactions occurring mainly in the mitochondria, peroxisomes and in the endoplasmic reticulum (Gorrini, Harris, and Mak 2013). It is estimated that about 2% of the oxygen consumed by mitochondria is reduced to from superoxide; mitochondria are therefore considered to be a major source of ROS (Finkel 2012; Handy and Loscalzo 2012). Peroxisomes are involved in both the scavenging of ROS (through catalase-mediated decomposition of H_2O_2) and in the production of ROS (through β-oxidation of fatty acids and flavin oxidase activity) (Schrader and Fahimi 2006). The endoplasmic reticulum constitutes an oxidizing environment that favors disulphide bond formation and protein folding, and increases ROS levels through protein oxidation (Malhotra and Kaufman 2007).

ROS are constantly produced by both enzymatic and non-enzymatic reactions. Enzyme-catalysed reactions that generate ROS include those involving NAD(P)H oxidase, xanthine oxidase, uncoupled endothelial nitric oxide synthase, arachidonic acid and metabolic enzymes such as the cytochrome P450 enzyme, lipoxygenase and cyclooxygenase. The mitochondrial respiratory chain is a non-enzymatic source of ROS (Gorrini, Harris, and Mak 2013).

The modulation of intracellular ROS levels is crucial for cellular homeostasis, as different ROS levels can induce different biological responses (Cairns, Harris, and Mak 2011; Sena and Chandel 2012). At low to moderate levels, ROS act as signalling molecules that sustain cellular proliferation and differentiation, and activate stress-responsive survival pathways (Janssen-Heininger et al. 2008). ROS can also act as inducers of pro-inflammatory cytokines (Naik and Dixit 2011) and the nuclear factor-κB (NF-κB) pathway (Gloire, Legrand-Poels, and Piette 2006). Specifically regarding the endothelium, it has been observed that under physiological conditions, ROS can act stimulating mitogenic and/or apoptotic pathways in vascular smooth muscle cells and endothelial cells (Irani 2000; Wolin, Gupte, and Oeckler 2002). On the contrary, an excessive ROS production damages cellular components such as DNA, proteins and lipid, leading to the well-known situation of "oxidative stress". Oxidative stress describes the condition wherein an excessive production of ROS overwhelms endogenous anti-oxidant defense mechanisms. So a tight regulation of both ROS producing (inducer) pathways and ROS-detoxifying (scavenger) pathways is required (Figure 13).

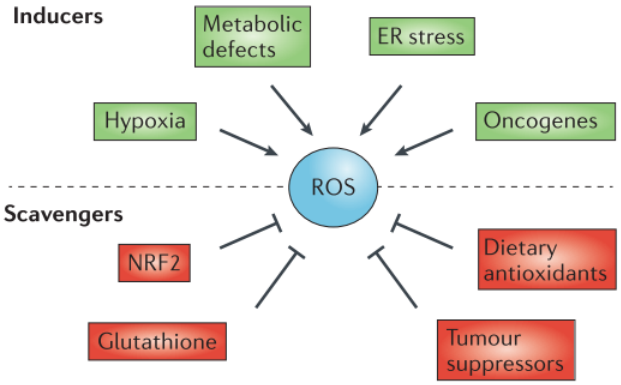

Figure 13: Determination of cellular redox status by a balance between levels of ROS inducers and ROS scavengers. The production of ROS can be induced by hypoxia, metabolic defects, ER stress and oncogenes. Conversely, ROS are eliminated by the activation of the transcription factor nuclear factor erythroid 2-related factor 2 (NRF2), the production of glutathione, the activity of tumour suppressors (such as breast cancer susceptibility 1 (BRCA1), p53, phosphatase and tensin homolog (PTEN) and ataxia telangiectasia mutated (ATM) and the action of dietary antioxidants (Gorrini, Harris, and Mak 2013).

An increasing body of evidence suggests that oxidative stress is involved in the pathogenesis of many cardiovascular diseases, including hypercholesterolemia, atherosclerosis, hypertension, diabetes, and heart failure (Basha et al. 2012; Elahi, Kong, and Matata 2009; Giacco and Brownlee 2010; Hink et al. 2001; Rashid, Sinha, and Sil 2013). The explanation is that the elevation in ROS levels has a detrimental effect on cellular functions, leading to important damages to lipid membranes, enzymes and nucleic acids (Cai and Harrison 2000).

Specifically, it has been largely demonstrated that diabetes mellitus and its derived cardiovascular complications are characterized by excess vascular production of ROS (Cai and Harrison 2000; Harrison et al. 2003) and oxidative stress. One of the earliest measurable causes of ROS overproduction and oxidative stress in diabetic subjects is hyperglycaemia. As explained before, hyperglycaemia induces increased superoxide anion production via activation of multiple pathways. Superoxide activates AGEs, PKC, polyol (sorbitol), hexosamine and stress-signaling pathways, leading to increased expression of inflammatory cytokines and vasoconstrictor factors sucha as angiotensin II and andothelin-1, which in turn generate more superoxide via multiple mechanisms. Hyperglycemia-induced superoxide generation might also favour increased expression of NOSs through the activation of NF-kB, which increases the generation of NO. Superoxide anion quenches NO, thereby reducing the efficacy of a potent endothelium-derived vasodilator system. Superoxide interacts with

NO to form the reactive oxidant peroxynitrite, which induces cell damage via lipid peroxidation, inactivation of enzymes and other proteins by oxidation and nitration and activation of matrix metalloproteinases. Peroxynitrite also acts on mitochondria to decrease the membrane potential and trigger the release of pro-apoptotic factors such as cytochrome c and apoptosis-inducing factor (AIF). These factors mediate caspase-dependent and -independent apoptotic death pathways. Peroxynitrite, in concert with other oxidants, causes strand breaks in DNA, activating the nuclear enzyme PARP-1. Mild damage to DNA activates the DNA repair machinery. By contrast, once excessive oxidative- and nitrosative stress-induced DNA damage occurs, overactivated PARP-1 initiates an energy-consuming cycle by transferring ADP-ribose units from NAD+ to nuclear proteins, resulting in rapid depletion of the intracellular NAD+ and ATP pools, slowing the rate of glycolysis and mitochondrial respiration, and eventually leading to cellular dysfunction and death. Poly(ADP-ribose) glycohydrolase (PARG) degrades poly(ADP-ribose) (PAR) polymers, generating free PAR polymer and ADP-ribose, which signals to the mitochondria to induce AIF release. PARP-1 activation also leads to the inhibition of cellular glyceraldehyde-3-phosphate dehydrogenase (GAPDH) activity which, in turn, favors the activation of PKC, AGEs and the hexosamine pathway, leading to increased superoxide generation. PARP-1 also regulates the expression of a variety of inflammatory mediators, which might facilitate the progression of diabetic cardiovascular complications (Pacher and Szabó 2006) (Figure 14).

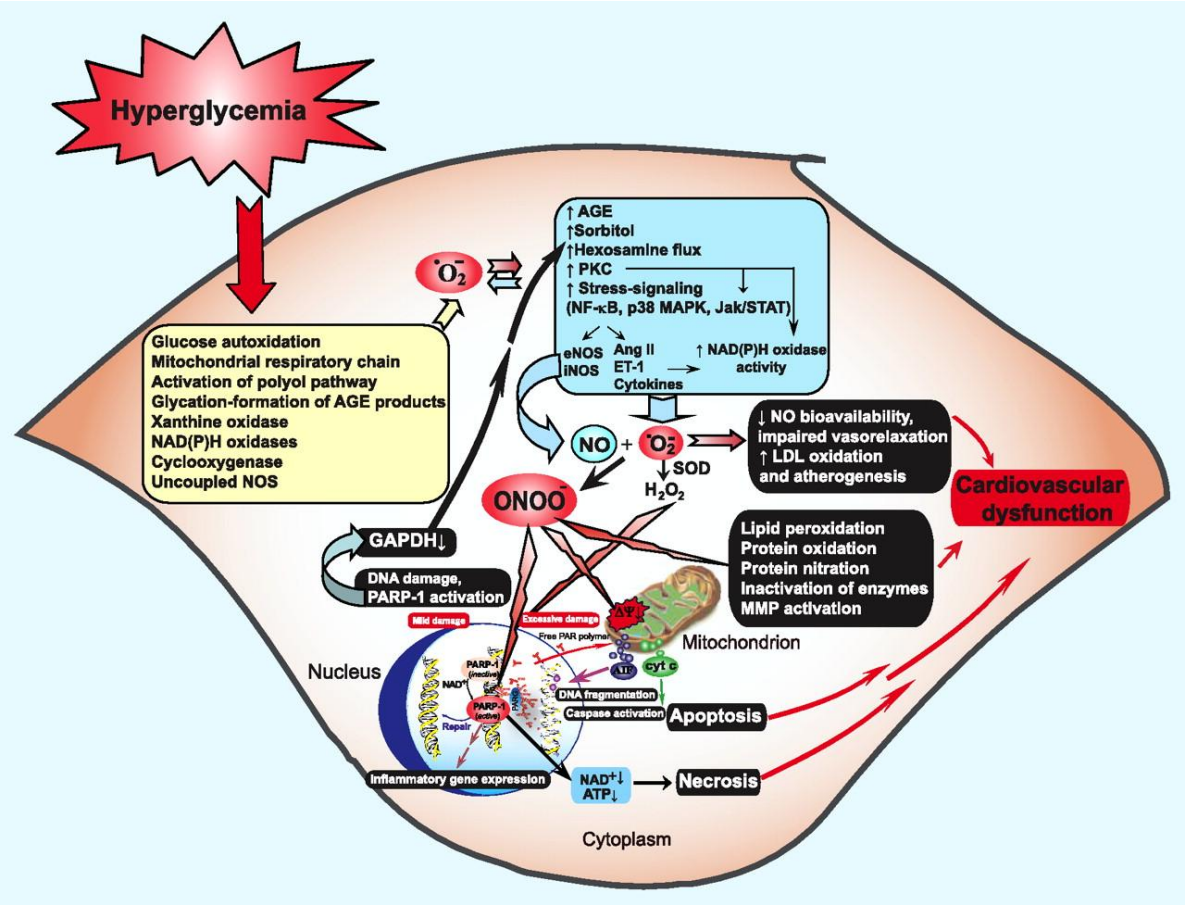

Figure 14: Mechanisms of cardiovascular dysfunction in diabetes: role of superoxide and peroxynitrite. Hyperglycaemia induces increased $\cdot O_2^-$ production via activation of multiple pathways. This favors an increased expression of eNOS through the activation of NF-κB, which may increase the generation of NO. Superoxide anion may quench NO, reducing its vasodilatory efficacy. Superoxide can also be converted to H2O2 by superoxide dismutase (SOD) and interact with NO to form a reactive ONOO-, which induces cell damage via lipid peroxidation, inactivation of enzymes and other proteins by oxidation and nitration, and activation of matrix metalloproteinases (MMPs) among others (Pacher and Szabó 2006).

6.1. General ROS inducers and ROS scavengers

Under physiological conditions, redox homeostasis is achieved by the constant balancing between ROS inducers and ROS scavengers (Figure 13).

6.1.1. ROS inducers

(i) Hypoxia. Hypoxia arises from an imbalance between oxygen supply and consumption. Major causes of hypoxic stress include a reduced presence or structural abnormality of microvessels supplying nutrients in a tissue, increased distance between the tissue and its nutrition-supplying blood flow and a reduced oxygen-transporting capacity of the blood owing to anaemia. Hypoxia is known to stimulate the production of ROS by mitochondria (Bell and Chandel 2007), and these ROS in turn activate hypoxia-inducible transcription factor 1 (HIF1) (Chandel et al. 1998). HIF1 is a heterodimeric transcription factor that promotes angiogenesis, survival, glycolysis and tumour progression (Semenza 2001).

(ii) Metabolic defects. Because ROS are by-products of metabolic reactions, altered metabolism can be a source of oxidative stress. Cancer cells have a high metabolic activity and require high levels of ATP to sustain their uncontrolled proliferation and growth. These two aspects result in sustained mitochondrial respiration, which leads to excessive ROS accumulation (Jones and Thompson 2009).

(iii) ER stress. The correct folding of proteins in the endoplasmic reticulum is essential for cell survival and normal physiological functions. The ER constitutes an oxidizing site where nascent proteins are engaged by the folding machinery to achieve the correct conformation and post-translational modifications. Misfolded proteins can elicit ER stress and the unfolded protein response (UPR), which eventually results in ROS accumulation (Kincaid and Cooper 2007). Mitochondrial ROS production can also be stimulated by ER stress-induced calcium release and depolarization of the mitochondrial inner membrane (Bravo et al. 2012).

(iv) Oncogenes. Previous studies have reported that oncogene activation increases ROS levels in cancer cells. For example, ectopic expression of MYC has been shown to lead to the upregulation of the expression of mitochondrial genes and increased ROS production (Tanaka et al. 2002). Similarly, ectopic expression of RAS and KRAS increases ROS levels through the regulation of NAD(P)H oxidase (Irani et al. 1997).

6.1.2. ROS scavengers

(i) NRF2. Normal cells counteract ROS by producing enzymes with antioxidant functions. Examples of these are phase II detoxification enzymes such as heme oxygenase (HMOX-1), NAD(P)H:quinone oxidoreductase 1 (NQO-1), glutathione S-transferases (GSTs) and UDP-glucuronosyltransferases (UGTs). The transcription factor nuclear factor erythroid 2-related factor 2 (NRF2) controls the expression of these enzymes and is considered to be a master regulator of intracellular antioxidant responses (W. Li and Kong 2009).

(ii) GSH. Glutathione (GSH) is the most abundant non-enzymatic antioxidant molecule in the cell and is essential for cell survival and redox homeostasis (Meister 1991). GSH synthesis is

catalysed by glutamate–cysteine ligase (GCL) and GSH synthase (GSS). Modification of GSH metabolism has been observed in many tumor types.

(iii) Tumor suppressors. Tumor suppressors such as forkhead box O (FOXO) transcription factors, retinoblastoma-associated protein RB and breast cancer susceptibility 1 (BRCA1) have been implicated in the control of oxidative stress (Vurusaner, Poli, and Basaga 2012). The role of the tumor suppressor p53 is more complex, as p53 has both pro-oxidant and antioxidant capacities (Vousden and Ryan 2009).

(iv) Dietary antioxidant compounds. Dietary antioxidants such as vitamin C, vitamin E, selenium and β-carotene are non-enzymatic systems that, although less specific than the enzymatic ones, appear to be equally important in cellular responses to oxidative stress (Bouayed and Bohn 2010). For example, vitamin C (ascorbic acid), which is mostly present in the cell in its redox form, ascorbate, acts as a reductant and enzyme cofactor (Wilson 2005). Vitamin E is considered a 'chain-breaking' antioxidant; it acts as a ROS scavenger by reacting with free radicals and converting these into tocopheryl radicals, thus lowering their radical damaging abilities (Brigelius-Flohe and Traber 1999). Selenium is a non-metal element that forms part of antioxidant selenoproteins such as glutathione peroxidase and thioredoxin reductase (Rayman 2005). β-carotene is the most abundant carotenoid in human diet. Its antioxidant property derives from its ability to quench singlet oxygen and trap peroxyl radicals (Burton and Ingold 1984).

7. ROS inducers and ROS scavengers in endothelium

In this section we center our attention in the mechanisms that are involved in ROS production and those that are responsible of antioxidant response and ROS scavenging in vasculature.

7.1. Source of ROS in the endothelium

Principal sources of ROS in the vasculature include NAD(P)H oxidase (Ray and Shah 2005; Soccio et al. 2005a), xanthine oxidase (H Cai and Harrison 2000) and the mitochondrial electron transport chain (Boveris, Oshino, and Chance 1972; Chance, Sies, and Boveris 1979; Ježek and Hlavatá 2005; Turrens 2003). In addition, "uncoupled eNOS" produces $\cdot O_2^-$ rather than NO under conditions of substrate (L-arginine) or co-factor (BH_4) deficiency (Forstermann and Munzel 2006; Vásquez-Vivar et al. 1998) (Figure 14). Other potential sources of ROS include arachidonic acid pathway enzymes, such as lipoxygenase and cyclooxygenase, cytochrome p450s, peroxidases and other hemeoproteins (Cai and Harrison 2000).

Here we report the major sources of ROS in the endothelium.

7.1.1. NAD(P)H Oxidase

NAD(P)H Oxidase (NOX) is the predominant source of $\cdot O_2^-$ in the human vasculature, catalyzing the one electron reduction of oxygen using nicotinamide adenine dinucleotide (phosphate) NADH or NAD(P)H as the electron donor (Soccio et al. 2005). The enzyme was originally characterized in neutrophils but it is present in VSMCs (Griendling et al. 1994; Ushio-Fukai et al. 1996) and endothelial cells (Bayraktutan et al. 1998; De Keulenaer et al. 1998; Mohazzab, Kaminski, and Wolin 1994).

Vascular NAD(P)H oxidase is a membrane-bound enzyme complex that can be found in different isoforms designated NOX1, NOX2, NOX3, and NOX4. It consists of membrane integrated cytochrome b558 and a number of cytosolic regulatory components: $p47^{phox}$, $p67^{phox}$, $p40^{phox}$ (where phox represents *ph*agocyte *ox*idase) and the GTP-binding protein, Rac1. The cytochrome b558 is itself comprised of two subunits, $p22^{phox}$ and nicotinamide adenine dinucleotide phosphate oxidase (NOX) protein, NOX2 ($gp91^{phox}$) or a functional isoform of this differentially expressed catalytic subunits: NOX1, NOX2, NOX3 or NOX4 (Ray and Shah 2005; Ushio-fukai et al. 1996) (Figure 15). Vascular NAD(P)H oxidase is a constitutive enzyme but can also be regulated in VSMCs by humeral factors such as Angiotensin II and a number of growth factors, including TNFα and platelet-derived growth factor (PDGF) (Ray and Shah 2005). In the endothelium, activity of the enzyme is upregulated by shear stress caused by increased blood flow (De Keulenaer et al. 1998).

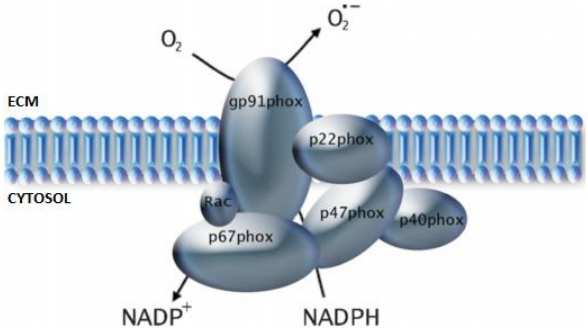

Figure 15: Structure of the active NAD(P)H oxidase complex. Vascular NAD(P)H oxidase is a heterodimer, consisting of membrane-bound p22phox and NOX subunits and cytoplasmic subunits, p67phox, p47phox and p40phox. Rac1 is required for assembly of the subunits. The NAD(P)H binding domain is predicted to be on one side of the membrane, while O^{2-} generation is predicted to occur on the other one (Ray and Shah 2005).

Vascular NAD(P)H oxidase-stimulated $\cdot O_2^-$ production has been shown to be positively correlated with endothelial dysfunction and clinical risk factors for CVD in humans (Guzik et al. 2000), while inhibition of the enzyme improves endothelial function in both rat and human blood vessels (Hamilton et al. 2002).

NAD(P)H oxidase NOX subunit expression is different among vascular cells. For example, endothelial cells predominantly express the NOX4 isoform and in a minority part NOX2 (Sorescu et al. 2002). Recent studies have demonstrated that NOX2 and NOX4-based NAD(P)H oxidases are the predominant contributors to oxidative stress in coronary arteries from patients with advanced cardiovascular artery disease (Guzik et al. 2006), while NOX5 has been identified as a novel, calcium-dependent source of ROS in these vessels (Guzik et al. 2008).

It has been shown that elevated $\cdot O_2^-$ production in human blood vessels from patients with T2DM is mediated by upregulated NAD(P)H oxidase activity (Guzik et al. 2002). Increased activity of the enzyme has also been implicated in the impaired endothelium-dependent vasodilation observed in the Otsuka Long Evans Tokushima Fatty (OLETF) rat, a useful animal model of T2DM with obesity (Kim et al. 2002). In addition, a number of *in vitro* studies have demonstrated that hyperglycaemia and AGE formation, characteristics of T2DM, increase NAD(P)H oxidase-induced $\cdot O_2^-$ production in endothelial cells (Ding, Aljofan, and Triggle 2007; Ulker et al. 2004; Weidig, McMaster, and Bayraktutan 2004). Furthermore, increased protein levels of $p22^{phox}$, $p47^{phox}$ and $p67^{phox}$ have been observed in human vessels from patients with T2DM (Guzik et al. 2002) while $p22^{phox}$ mRNA was shown to be up-regulated in vessels from streptozotocin-induced diabetic and OLETF rats (Kanie and Kamata 2002; Kim et al. 2002).

The specific mechanisms underlying enhanced NAD(P)H oxidase activity in T2DM are yet to be fully elucidated but recent studies have indicated a crucial role for PKC. PKC is a recognized stimulant of NAD(P)H oxidase activation and it is increased in conditions of hyperglycaemia (Wautier et al. 2001; Yan et al. 1994).

7.1.2. Endothelial Nitric Oxide Synthase

Nitric oxide, first identified as endothelium-derived relaxing factor (Ignarro et al. 1987; Palmer, Ferrige, and Moncada 1987), is a potent signalling molecule and vasodilator, responsible for mediating many functions of the endothelium, including control of vascular tone, inhibition of platelet aggregation and leukocyte adhesion and suppression of vascular smooth muscle cells proliferation (Cockcroft 2005; Moncada and Higgs 2006; Yetik-Anacak and Catravas 2006). Each of these events has been implicated in the initiation and progression of atherosclerosis, so that NO is considered an anti-atherosclerotic agent (Forstermann and Munzel 2006b; Moncada and Higgs 2006a).

NO is synthesized from the guanidino group of L-arginine and can be produced by almost all mammalian cells, including endothelium, neurons and cells from the immune system (Kubes 2000). NO is produced by three distinct enzyme systems: (i) the constitutive endothelial nitric oxide synthase found in the vasculature (eNOS); (ii) the constitutive nitric oxide synthase found in neurons from the brain and the enteric nervous system (nNOS) and (iii) the inducible nitric oxide synthase (iNOS) (Kubes 2000) .

Here we focus our attention to eNOS (also known as NOS3). Vascular NO formation requires Ca^{2+}/calmodulin, flavin adenine dinucleotide (FAD), flavin mononucleotide (FMN), NAD(P)H and tetrahydrobiopterin (BH_4) as cofactors (Moncada and Higgs 2006; Palmer et al. 1988; Yetik-Anacak and Catravas 2006). eNOS is activated in response to elevated cytosolic Ca^{2+} which occurs following the exposure to various stimuli, including shear stress. In addition, eNOS is known to be activated by hormones, for example insulin, and platelet-derived substances and agonists, such as bradykinin and acetylcholine (Kawashima and Yokoyama 2004; Moncada and Higgs 2006). It has recently been demonstrated that eNOS is regulated by reversible phosphorylation and both AKT and 5' adenosine monophosphate-activated protein kinase (AMPK) have been shown to phosphorylate and activate eNOS at Serine 1177 in cultured endothelial cells (Michell et al. 1999; Morrow et al. 2003).

Once produced and released from endothelial cells, NO diffuses rapidly through tissue and across cell membranes and binds to its most sensitive known target, soluble guanylate cyclase (sGC), to stimulate the production of cyclic GMP, which in turn activates protein kinase G (PKG), leading to reduced intracellular calcium and vasodilation (Isenberg et al. 2009). This regulates a number of signalling pathways that affect vascular cell function (Figure 16).

Given its cardioprotective function and its fundamental role in maintaining vascular homeostasis, loss of endothelial NO bioavailability is a maladaptive event and represents a common manifestation of endothelial dysfunction (Forstermann and Munzel 2006; Kawashima and Yokoyama 2004; Yetik-Anacak and Catravas 2006).

Reduction of NO bioavailability in the endothelium may be the result of impaired NO production due to reduced expression of eNOS (Wilcox et al. 1997), lack of substrate or cofactor (Vásquez-Vivar et al. 1998) or alterations in cellular signalling leading to reduced eNOS activation (Shimokawa, Flavahan, and Vanhoutte 1991). However, the reduced endothelial NO bioavailability associated with CVD has been reported to occur as a consequence of elevated ROS production under conditions of oxidative stress (Cai and Harrison 2000). In this situation, eNOS may generate $\cdot O_2^-$ rather than NO, a phenomenon termed “uncoupled eNOS” (see Figure 14). Nitric oxide generation depends on eNOS homodimerization in the presence of BH_4. However, BH_4 is highly susceptible to oxidative degradation by $ONOO^-$ and in the absence of its cofactor, eNOS fails to dimerize fully, resulting in uncoupling of the enzyme and amplification of oxidative stress (Milstien and Katusic 1999).

Uncoupled eNOS has been shown to contribute to increased superoxide production and endothelial dysfunction in a number of CVDs, including T2DM (Kawashima and Yokoyama 2004; Moncada and Higgs 2006).

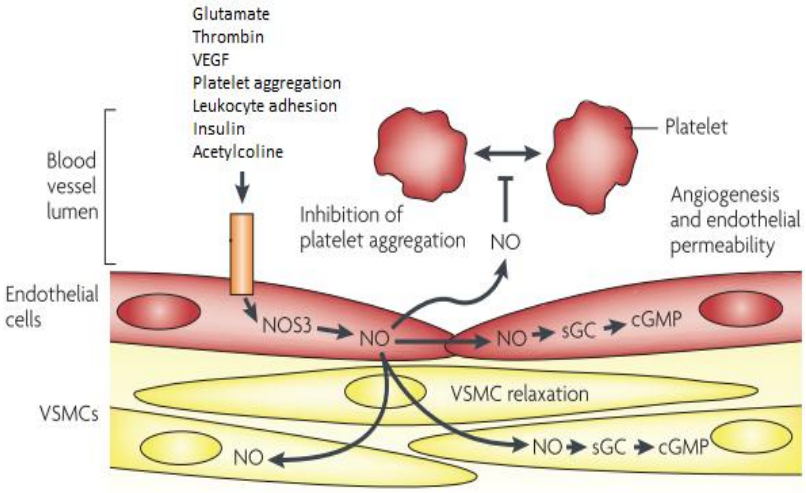

Figure 16: The central role of NO signalling in angiogenesis, vascular tone and hemeostasis. Vascular endothelial growth factor A (VEGFA) binding to its receptor VEGFR2 activates eNOS to produce NO. NO acts in an autocrine manner to stimulate ECs growth and motility leading to angiogenesis. VEGFA signalling through NO also contributes to increasing vascular permeability. NO diffuses into vessel walls, causing arterial vessels to relax and increase blood flow. NO also acts in a paracrine manner to prevent thrombosis by inhibiting platelet adhesion and aggregation (Isenberg et al. 2009).

7.1.3. Mitochondria

The oxidative phosphorylation (OXPHOS) pathway is essential for energy production in mitochondria of eukaryotic cells. Enzymes of the inner mitochondrial membrane transfer electrons along the electron transport chain (ETC) generating a proton gradient and enabling ATP synthase to generate ATP. Under physiological conditions, this process produces mitochondrial ROS (mtROS) as "byproducts", a result of the one electron reduction of oxygen to superoxide (Ballinger 2005; Murphy 2009). For this, a network of mitochondrial antioxidant systems has been developed in order to protect against ROS-induced damage to mitochondrial proteins, lipids and nucleic acids (Figure 17), as it has been explained in the paragraph 7.2 of this Section.

However, under conditions of oxidative stress, these antioxidant systems are overwhelmed, allowing mtROS to exert their damaging effects and ultimately alter mitochondrial function (Ballinger 2005; Turrens 2003). Increased production of mtROS leads to damage of mitochondrial DNA (mtDNA) and progressive mitochondrial dysfunction, and it has been shown to be associated with vascular diseases (Corral-Debrinski et al. 1992). Increased levels of mtROS are implicated in processes that are known to contribute to the pathogenesis of diabetic macrovascular disease, including PKC activation and AGEs formation (Ballinger 2005; Madamanchi and Runge 2007; Nishikawa et al. 2000; Zhang and Gutterman 2007) (Figures 5 and 18). In addition, the elevated free fatty acids (FFAs) flux and oxidation, a characteristic of visceral obesity and insulin resistance, are known to induce mtROS production in ECs (Du et al. 2006) (Figure 18).

Mitochondrial ROS have a fundamental role in the development and progression of endothelial dysfunction and macrovascular disease in T2DM, with hyperglycaemia shown to increase generation of $\cdot O_2^-$ from the mitochondrial ETC in ECs (Nishikawa et al. 2000). Intracellular hyperglycaemia causes an increase in the mitochondrial proton gradient, a consequence of electron donor (NADH and $FADH_2$) overproduction by the citric acid cycle, also known as the tricarboxylic acid (TCA) cycle or citrate cycle. This, in turn, leads to increased mitochondrial production of ROS (Figure 18).

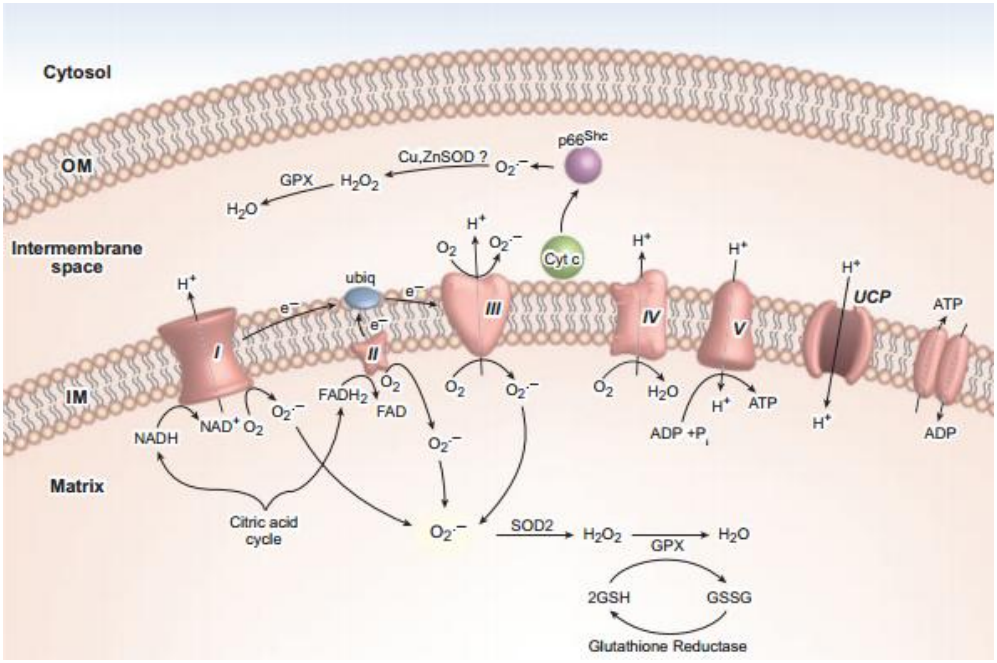

Figure 17. Oxidative phosphorylation, superoxide production and scavenging pathways in mitochondria. Electrons from NADH and $FADH_2$ pass through complex I, II and III via ubiquinol. Cytochrome c transfers electrons from complex III to complex IV, which reduces $\cdot O_2^-$ to form H_2O. Flow of electrons is accompanied by proton transfer across the inner mitochondrial membrane at complexes I, III, and IV, creating an electrochemical gradient. Protons reenter the mitochondrial matrix through complex V, which uses the proton-motive force to generate ATP. UCPs allow protons to return to the matrix, reducing ROS formation. $p66^{Shc}$ in the intermembrane space subtracts electrons from cytochrome c to produce O_2^-. Superoxide is dismutated to H_2O_2 by Cu, ZnSOD in intermembrane space and by SOD2 in the matrix. H_2O_2 is reduced to H_2O by GPX using GSH, and the resultant oxidized glutathione (GSSG) is reduced back to GSH by glutathione reductase (Madamanchi and Runge 2007).

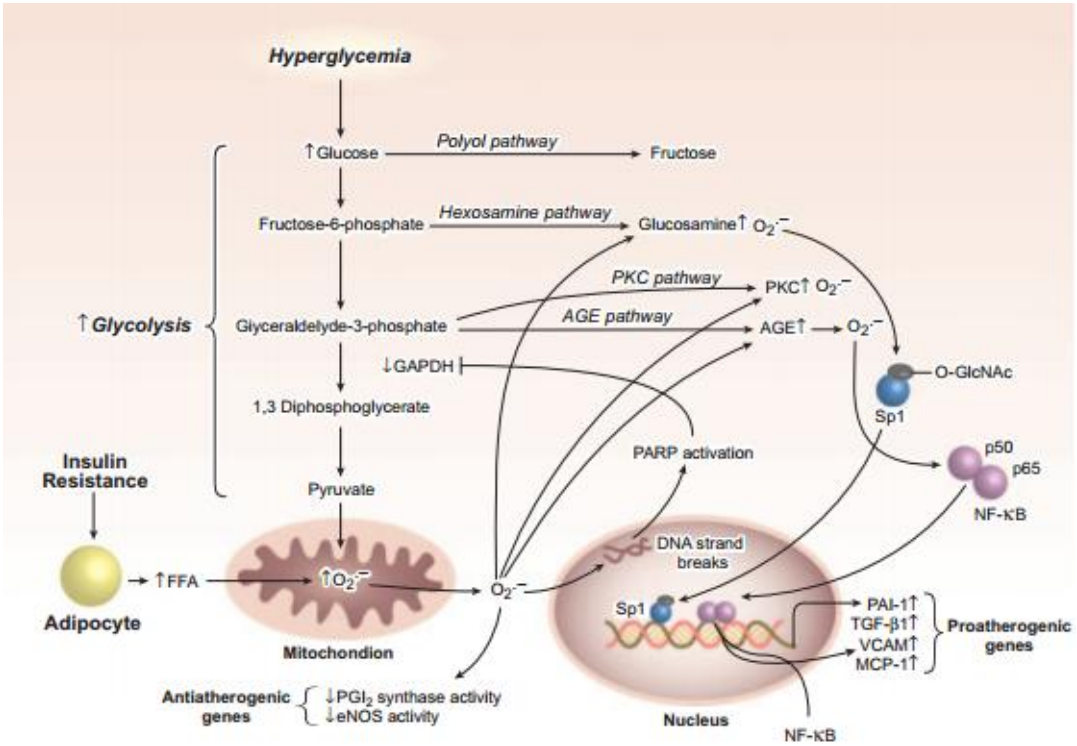

Figure 18. Hyperglycaemia-induced increased mitochondrial superoxide production as well as insulin resistance activate atherogenic signalling pathways. Overproduction of $\cdot O_2^-$, caused by high glucose, results in the activation of poly (ADP ribose) polymerase (PARP). PARP ribosylates and blocks GAPDH. The upstream metabolites of disrupted glycolytic pathway are processed through polyol pathway, hexosamine pathway, PKC pathway, or AGE pathway. Glycosylation of transcription factor Sp1 causes transactivation of the atherogenic genes PAI-1 and TGF-β1. Activation of NF-kB induces transactivation of VCAM-1 and MCP-1. Increased flux of FFAs also activates hexosamine, PKC, and AGE pathways, and in addition, inactivate the antiatherogenic enzymes PGI2 synthase and eNOS (Madamanchi and Runge 2007).

7.2. ROS endothelial scavengers and the antioxidant response against oxidative stress

A number of endogenous anti-oxidant defense mechanisms, both enzymatic and non-enzymatic, operate to limit ROS levels in the vasculature. Non-enzymatic anti-oxidant molecules include ascorbic acid (vitamin C), α-tocopherol (vitamin E) and glutathione, while superoxide dismutases (SODs), catalase (CAT) and glutathione peroxidases (GPXs) represent important anti-oxidant enzymes which act to directly scavenge ROS, converting them to less reactive species (Li and Shah 2004).

7.2.1. Superoxide Dismutase (SOD)

The SODs represent the first and most important line of enzymatic anti-oxidant defense against ROS. A ubiquitous family of enzymes, SODs catalyze the conversion of $\cdot O_2^-$ to H_2O_2 and O_2 (Zelko, Mariani, and Folz 2002) (Figure 19).

Three distinct isoforms of SOD have been identified in vascular tissue. The first isoform, cytosolic copper/zinc SOD (Cu/ZnSOD), is an unusually stable homodimer encoded by the SOD1 gene. SOD1 is believed to be the predominant SOD isoform in the endothelium and is thought to lower $\cdot O_2^-$ concentrations from the nanomolar to picomolar range (Zelko, Mariani, and Folz 2002). A second isoform, encoded by SOD2, is localized in mitochondria, and functions as a homotetramer and utilizes manganese (Mn) as cofactor (Zelko, Mariani, and Folz 2002). SOD3 encodes the extracellular SOD (ecSOD), a copper/zinc-containing tetramer which has a C terminal heparin-binding region, which is principally located in arterial smooth muscle cells in the vascular wall (Zelko, Mariani, and Folz 2002).

The importance of SODs as an anti-oxidant defense mechanism has been highlighted by gene transfer studies wherein SOD overexpression improved endothelial function (Fennell et al. 2002; Zanetti et al. 2001) and provided protection against myocardial infarction (Li et al. 1998). Overexpression of SOD2 has also been shown to prevent hyperglycaemia-associated production of $\cdot O_2^-$, activation of PKC and AGEs formation (Nishikawa et al. 2000), supporting a role for mtROS production in diabetic CVD.

7.2.2. Catalase (CAT)

Catalase is the homotetrameric heme-containing enzyme principally responsible for H_2O_2 metabolism following dismutation of $\cdot O_2^-$ by SOD (Li and Shah 2004). An intracellular anti-oxidase, catalase is primarily located in peroxisomes, but also functions in the cytosol and catalyzes the conversion of H_2O_2 to H_2O and O_2 (Li and Shah 2004) (Figure 19).

Inherited catalase deficiency has been linked to elevated cardiovascular risk and increased incidence of diabetes in affected families (Leopold and Loscalzo 2005). However, experimental investigation has provided evidence that catalase affords only moderate protection against oxidative stress (Muzykantov 2001) and while gene transfer studies showed reduced ROS production on co-expression of SOD and CAT, the relative contribution of each gene was not ascertained (Durand et al. 2005).

7.2.3. Glutathione Peroxidases (GPXs)

Glutathione, a tripeptide comprised of glutamate, cysteine and glycine, is the principal low molecular weight non-protein thiol in the cell (Li and Shah 2004). Mainly found in the reduced state,

glutathione has numerous functions in metabolism, signal transduction and gene expression (Wu et al. 2004). GSH acts as an electron donor and can directly scavenge ROS, but also acts as a cofactor in the conversion of H_2O_2 to H_2O by glutathione peroxidases (Li and Shah 2004).

The GPXs are a family of tetrameric enzymes with a role in both first and second line of antioxidant defense. Like catalase, GPXs act to reduce the H_2O_2 produced as a result of the dismutation of H_2O_2 by SOD, transferring electrons from GSH to H_2O_2 with the subsequent formation of H_2O and O_2 and conversion of GSH to oxidized glutathione disulphide (GSSG) (Li and Shah 2004) (Figure 19).

There are four known GPX isoforms, each containing selenocysteine at the active site (Leopold and Loscalzo 2005).

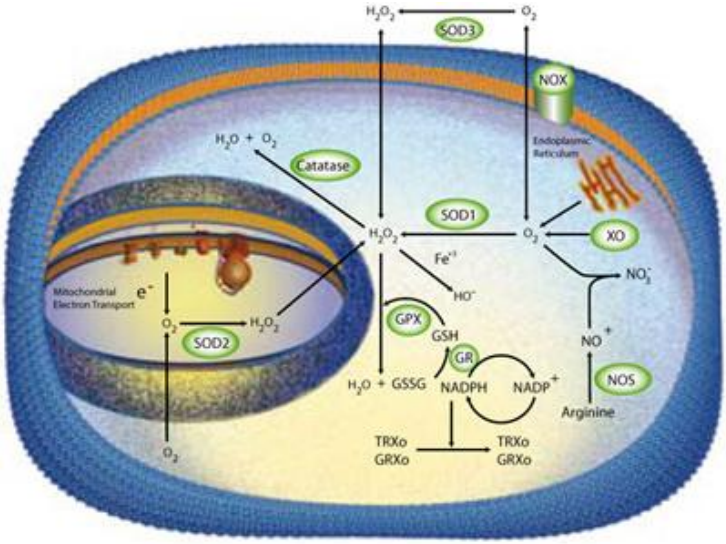

Figure 19: ROS scavengers as mechanism to counteract oxidative stress. Oxidative stress is implicated in the pathogenesis of lipotoxicity in both animal and human studies. Multiple enzymatic scavengers are utilized by the cell to limit damage from reactive oxygen species. These scavengers include members of the superoxide dismutase (SOD) family, catalase, and glutathione peroxidase (GPX) (http://www.sigmaaldrich.com/technical-documents/articles/biofiles/mitochondrial-stress-and-ros.html).

8. Modulators of the antioxidant response in endothelium

There are numerous regulators, both positive and negative, that play an important role in the expression of antioxidant genes (Gorrini, Harris, and Mak 2013). In endothelium as well as in other cellular tissues, the major modulators of antioxidant defense system, that respond under oxidative stress conditions, are the transcription nuclear factor erythroid 2- related factor 2 (NRF2), the forkhead box O (FOXO) family and the tumor suppressor p53.

8.1. NRF2

NRF2 is the most important regulator of the expression of many genes involved in cytoprotective and antioxidant responses (Gorrini, Harris, and Mak 2013).

In normal conditions NRF2 interacts with the ubiquitination adapter protein Kelch-like ECH-associated protein 1 (KEAP1), which targets NRF2 for proteosomal degradation (Nguyen, Nioi, and Pickett 2009). Contrary, oxidative stress induces stabilization of NRF2 in the nucleus, where it heterodimerizes with the ubiquitous bZIP protein MAF. Then, it is translocated into the nucleus where it binds to antioxidant responsive elements (ARE, also called electrophile response elements, EpRE) in regulatory regions of Nrf2-response genes (Nguyen, Nioi, and Pickett 2009), modulating basal and inducible expression of antioxidant and detoxification enzymes. NRF2 targets are involved in glutathione synthesis, ROS elimination, xenobiotic metabolism and drug transport. Among them the most studied are: heme oxygenase 1 (HMOX-1), NAD(P)H:quinone oxidoreductase 1 (NQO-1),

thioredoxin reductase (TXNRD) and thioredoxin interacting protein (TXNIP) (He and Ma 2012; Pecorelli et al. 2013).

Loss of Nrf2 gene expression completely ablates the induction of Nrf2 target genes, rendering $Nrf2^{-/-}$ mice susceptible to high levels of oxidative stress, including the intake of toxins and the exposure to carcinogens (Chan and Kwong 2000). Additionally, $Nrf2^{-/-}$ mice display a modest decrease in life expectancy, an effect that is thought to result from improper ROS detoxification (Yoh et al. 2001). Disruption of KEAP1 activates the NRF2 pathway and results in increased resistance to oxidative challenges (Okawa et al. 2006). Thus, the NRF2 pathway provides a rapid feedback triggered mechanism of countering oxidative challenges (Suvorova et al. 2009).

Nrf2 is ubiquitously expressed in the vasculature. Here, we have reported the functions of selected target genes and their roles in vascular biology and pathogenesis.

8.1.1. Heme oxygenase-1 (HMOX-1)

HMOX-1 is an enzyme involved in heme degradation that has multiple protective effects. During cellular homeostasis its activity is repressed by the binding with BACH1. Under stress conditions HMOX-1 is induced and strictly regulated by NRF2. Both the repression in basal conditions and inducible expression during cellular stress are mediated by the two ARE regions, the proximal and distal enhancers (Alam et al. 1999), which are controlled by both BACH1 and NRF2, binding the distal ARE with higher affinity and in a reciprocal manner (Reichard, Motz, and Puga 2007). In addition to the NRF2-ARE pathway, other transcription factors and regulatory elements take part in the inducible expression of HMOX-1 (Alam et al. 1999).

HMOX-1 catalyzes a reaction in which heme is metabolized to biliverdin and further to bilirubin by biliverdin reductase. The reaction also produces carbon monoxide (CO) and iron. CO plays an important role as an anti-inflammatory and antiapoptotic molecule in vascular cells, preventing platelet aggregation and inhibiting apoptosis of endothelial cells and fibroblasts. The free iron released in the reaction is stored as ferritin. Bilirubin is an important antioxidant that has a role as a scavenger of lipid peroxides (Otterbein et al. 2003).

Polymorphisms of human HMOX-1 promoter guanine-thymine-repeats are associated with cardiovascular diseases. Studies in the Japanese population showed that the lengthening of guanine-thymine-repeats in the presence of other risk factors associates with increased prevalence of atherosclerosis (Kaneda et al. 2002).

8.1.2. NAD(P)H: quinone oxidoreductase-1 (NQO-1)

NQO-1 is often referred to a classical NRF2-dependent gene (Nioi and Hayes 2004). NQO-1 gene expression is regulated via NRF2-ARE pathway in basal conditions as well as during oxidative stress. NRF2 deficiency impairs the constitutive expression of NQO-1 and inhibits its induction (Nioi and Hayes 2004).

NQO-1 is quinone detoxifying enzyme that has a function in recycling cellular antioxidants, vitamin E and ubiquinone, after radical attacks. Ubiquinone and vitamin E play an important role as liposoluble antioxidants that protect cells against lipid peroxides (Nioi and Hayes 2004).

NQO-1 also plays a role in stabilizing p53 by inhibiting its degradation. Actually, $Nqo\text{-}1^{-/-}$ mice express lower levels of p53 compared with controls (Long et al. 2002). These studies demonstrate the important role of NQO-1 in cancer prevention (Nioi and Hayes 2004).

Recently, it has been proposed also a role for NQO-1 in the development and progression of atherosclerosis via regulation of smooth muscle cells proliferation. Pharmacological induction of NQO-1 has been shown to prevent arterial restenosis via inhibition of SMCs proliferation (Kim et al. 2009). In this sense, it has also been demonstrated that single nucleotide polymorphisms in NQO-1 lead to a decreased level of functional protein and are associated with carotid artery plaques in T2DM patients (Han et al. 2009).

8.1.3. Thioredoxin (TXN) and Thioredoxin Reductase (TXNRD)

Expression of Thioredoxin (Txn/Trx) and Thioredoxin reductase (Txnrd) genes are both regulated via NRF2-ARE pathway (Kim et al. 2001).

TRXs are ubiquitously expressed and highly conserved antioxidant enzymes that reduce oxidized thiol groups in proteins. There are two members of the TRX family: cytoplasmic and nuclear TRX-1, and mitochondrial TRX-2. Both forms have a critical -Cys-Gly-Pro-Cys- site, which is essential for reduction-oxidation function. During the reduction of proteins, TRX itself oxidizes and is reduced by TXNRD in an NAD(P)H-dependent reaction (Holmgren and Lu 2010) (Figure 20).

Cytosolic TRX-1 regulates proliferation and apoptosis signalling pathways by controlling interactions of TRX-binding proteins (Saitoh et al. 1998). For example, TRX-1 is an important inhibitor of apoptosis signalling kinase 1 (ASK-1) (Saitoh et al. 1998) (Figure 20). If the activity of TRX-1 is inhibited, TNF-α phosphorylates ASK-1, leading to the activation of downstream p38 and Jun-terminal kinase (JNK) (Ichijo et al. 1997). Downstream kinases mediate the expression of adhesion and inflammatory genes, such as VCAM-1.

TRX-1 also has a redox-regulatory activity, playing a role in controlling signalling pathways that are involved in ROS production in endothelium. One mechanism is the modification of Cys69 by NO that leads to increased TRX-1 activity, with the consequent reduction of intracellular ROS and inhibition of apoptosis (Haendeler et al. 2004).

Recently, it has been proposed that mitochondrial TRX-2 also plays a role in cardiovascular diseases because its function is similar to that of TRX-1 (Dai et al. 2009).

8.1.4. Thioredoxin Interacting Protein (TXNIP)

TXNIP (also termed vitamin D-upregulated protein 1, VDUP1) inhibits TRX-1 activity in a redox-dependent manner by binding reduced TRX-1 but not oxidized TRX-1 (Nishiyama et al. 1999). In normal conditions TXNIP is down-regulated, and this favors the cytoprotective effects of TRX-1. In contrast, under stress conditions TXNIP expression is induced and this leads to the formation of TRX-1-TXNIP complex, which results in the release of ASK-1 from TRX-1, with the subsequent activation of pro-apoptotic and pro-inflammatory pathways (Yamawaki et al. 2005) (Figure 20).

The transcriptional regulation of TXNIP is mainly studied in pancreatic and cancer cell lines, where it is regulated via multiple transcription factors and stimuli. As referred to endothelium, it has been demonstrated that in human aortic endothelial cells (HAECs) TXNIP expression is induced in a glucose mediated manner by the forkhead O1 transcription factor (FOXO1), which leads to increased ROS production (Li et al. 2009). In smooth muscle cells it has been shown that TXNIP is down-regulated by NO, (Schulze et al. 2006). NO also induces protein S-nitrosylation via transcriptional repression of TXNIP, thus releasing TRX-1 (Forrester et al. 2009) and supporting the protective role of NO in the vascular wall.

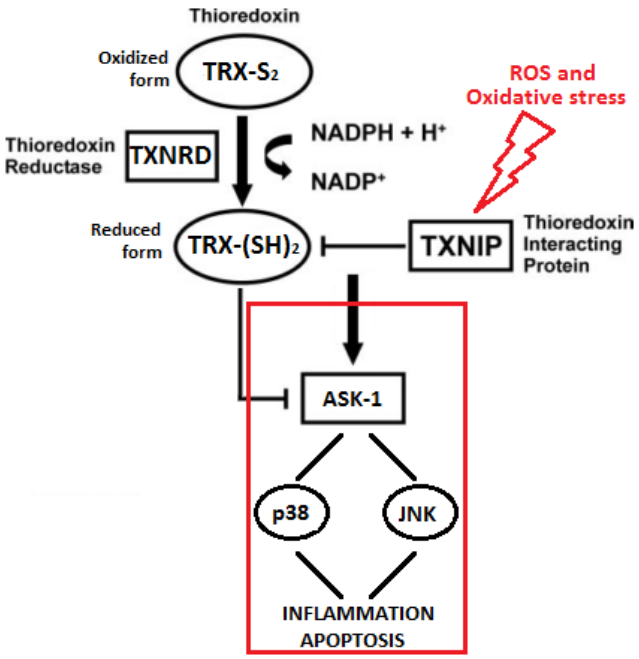

Figure 20: Thioredoxin system and its related pathway. During the reduction of proteins, TRX oxidizes itself and then is reduced by TXNRD in an NAD(P)H-dependent reaction. Under normal conditions, cytoplasmic TRX-1 has pro-proliferative and anti-apoptotic properties by inhibiting, for example, ASK-1 signalling pathway. Hyperglycemia promotes the formation of ROS and oxidative stress upregulates TXNIP, which in turn inhibits TRX-1 activity in a redox-dependent manner by binding reduced TRX-1. This leads to the formation of TRX-1-TXNIP complex, which results in the release of ASK-1 from TRX-1, with the subsequent activation of pro-apoptotic and pro-inflammatory pathway.

In synthesis, TRX controls levels of ROS and limits damage from oxidative stress. TXNIP is an oxidative stress mediator that acts by inhibiting TRX activity (Patwari et al. 2006). TXNIP may have an important role in diabetes (Yoshihara et al. 2013), for example it is the most significantly upregulated gene in response to glucose isolated pancreatic islet cells (Zhao, Li, and Tang 2015). Inhibition of TRX by TXNIP carriers lethal consequences for the cell (Zhao, Li, and Tang 2015). It has been shown that TXNIP induction plays a critical role in impaired angiogenesis (Schulze et al. 2004). Free TXNIP that has dissociated from TRX activates the machinery of inflammasome leading to the release of Caspase 1 and Interleukin 1β, resulting in death of pancreatic β-cells, endothelial cells and intraocular vessels (Chong et al. 2014). Multiple observations in animal models have demonstrated an increase in a diabetic-like environment, especially in blood vessel walls (Berk 2007). The overexpression of TXNIP in presence of hyperglycaemia may have deleterious effects by increasing the development of atherosclerotic disease (Perrone et al. 2009).

8.2 The FOXO family and p53

Although primarily known as inducers of cell cycle arrest and cell death, the FOXO family of transcription factors and the tumor suppressor p53 also play an important role in counteract ROS overproduction and oxidative stress by inducing the antioxidant gene expression (Gorrini, Harris, and Mak 2013).

FOXO transcription factors are activated by auto-phosphorylation, this leads to their binding with the 14-3-3 protein (also known as YWHAQ), which in turn triggers their nuclear exclusion and cytoplasmic sequestration (Brunet et al. 2001; Kops et al. 1999).

The role of FOXO transcription factors in oxidative stress is controversial: there are reports showing that FOXOs can be activated by JNK and macrophage stimulating protein 1 (MST1); and others demonstrating that can be inhibited by AKT, in a condition of ROS overproduction (Gorrini, Harris, and Mak 2013).

FOXO transcription factors are involved in the regulation of multiple pathways (Gorrini, Harris, and Mak 2013):

1. glutathione-mediated detoxification by inducing the transcription of Gpx1 and Glutathione S-transferase Mu1 (Gstm-1);
2. Fe(ii) homeostasis by inducing the transcription of Hmox-1;
3. mitochondrial function via PTEN-induced putative kinase (Pink-1).

Also they directly exert their antioxidant effects through the regulation of SODs and CAT (Gorrini, Harris, and Mak 2013). In addition, FOXO transcription factors up-regulate cyclin-dependent kinase inhibitor 1A (CDKN1A; also known as p21 or WAF1), which promotes NRF2 stabilization (W. Chen et al. 2009).

The final transcription factor that exerts an important role in the regulation of antioxidant gene expression is p53 (Gorrini, Harris, and Mak 2013). p53 has a controversial role in ROS regulation as it has been demonstrated that can promote both pro- and antioxidant responses (Vousden and Ryan 2009). The pro-oxidant role of p53 is essentially mediated by cell death pathways (Shi et al. 2012).

As concern as its antioxidant properties, an important target of p53 is the TP53-induced glycolysis and apoptosis regulator (TIGAR) (Bensaad et al. 2006). TIGAR encodes a protein that is similar to the glycolytic enzyme fructose-2,6-bisphosphatase, which degrades fructose-2,6-bisphosphate (Fru-2,6-P_2). A decrease in Fru-2,6-P_2levels inhibits the activity of the rate-limiting enzyme phosphofructokinase 1 (PFK1), blocking glycolysis and promoting the shuttling of metabolites to the Pentose phosphate pathway (PPP). By upregulating TIGAR, p53 amplifies PPP-mediated NADPH production.

Another important antioxidant target of p53 is glutaminase 2 (GLS2) (Suzuki et al. 2010). The tight control of GLS expression is essential for the synthesis of GSH (Gorrini, Harris, and Mak 2013).

Together, FOXO transcription factors and p53 have complementary functions in the antioxidant response: for example, p53 promotes GSH production through GLS2, whereas FOXO transcription factors promote GSH-mediated detoxification via GPX1 and GSTM1. Moreover, FOXOs control distinct and overlapping antioxidant genes that are not regulated by NRF2 (Figure 21): for one hand NRF2 promotes NAD(P)H- and GSH-mediated detoxification and also thioredoxin-mediated peroxide detoxification and disulphide reduction via TXNRD; for the other hand FOXO transcription factors control SODs and CAT. In addition, both FOXO transcription factors and p53 upregulate CDKN1A, which promotes NRF2 stabilization (W. Chen et al. 2009). NRF2, FOXO and p53 also promote HMOX-1 expression (Alam et al. 1999; Cheng et al. 2009; Meiller et al. 2007).

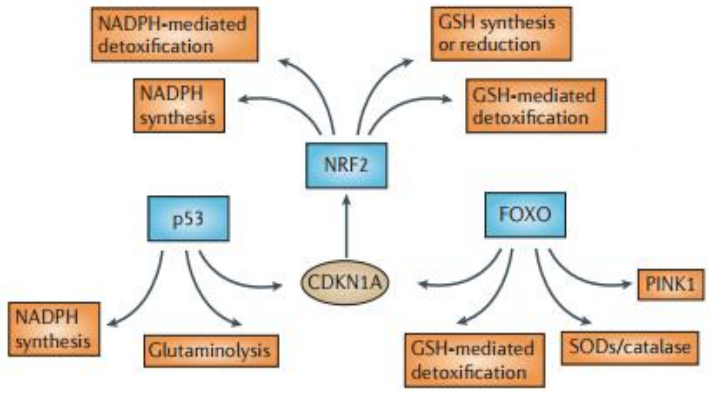

Figure 21: The antioxidant pathways of the modulators NRF2, FOXOs and p53. NRF2 mainly control GSH- and NAD(P)H-related responses. FOXOs proteins are involved in the control of SODs and catalase, PINK1 and, as well as NRF2, GSH-mediated detoxification. p53 promotes glutaminolysis via GLS2, which produces the glutamate required for GSH synthesis and also is involved in NAD(P)H synthesis. In addition, both FOXOs and p53 control NRF2 stabilization via the expression of CDKN1A (Gorrini, Harris, and Mak 2013).

9. Endoplasmic reticulum stress and diabetes mellitus

During the last decade, endoplasmic reticulum stress has emerged as a new player in the pathogenesis of diabetes and a considerable number of recent studies have pointed out its role in the onset of insulin resistance and hyperglycaemia (Cnop, Foufelle, and Velloso 2012).

9.1. Basical functions of ER

The endoplasmic reticulum is an extensive membrane network that plays several functions essential for cell homeostasis and the whole organism. It is responsible for the synthesis and folding of proteins that traffic through the secretory pathway or that are anchored into membranes. Secreted and transmembrane proteins, newly translated as unfolded polypeptide chains, are translocated into the ER, which is equipped with chaperones and folding enzymes in an oxidizing and Ca^{2+}-rich environment (Cnop, Foufelle, and Velloso 2012). Nascent polypeptides are then folded into secondary and tertiary structures that are stabilized by disulfide bonds formed with the assistance of protein disulfide isomerase. Mature proteins that pass quality control are then exported to the Golgi and finally liberated into the cytoplasm of exposed to the membrane.

ER is also the site at which all the posttranslational modifications (N-glycosylation and oligomerization) required for protein functions take place. Thus, the ER represents a protein folding factory with strict quality control of proteins, which guarantees that only correctly matured proteins are exported through the secretory pathway but also that misfolded proteins leave the ER to be ubiquitinated and degraded by the proteasome through a process known as ER-associated degradation (ERAD).

Protein folding is Ca^{2+}-dependent and one of the important functions of the ER is Ca^{2+} storage and signalling. The Ca^{2+} concentration in the ER is orders of magnitude higher than in the cytosol, and this gradient is generated by the sarco(endo)plasmic reticulum Ca^{2+} ATPase (SERCA) pump.

The ER is also involved in the biosynthesis of cholesterol, phospholipids, triglycerides, steroids and lipid second messengers (ceramides). Finally it plays a crucial role in the assembly of very low density lipoprotein (VLDL) in the liver, and in lipid droplet formation in adipocytes (Flamment et al. 2012).

9.2. The canonical Unfolded Protein Response

Under pathological conditions that perturb ER homeostasis, such as overexpression of misfolded proteins, as well as insufficient ER chaperone levels or Ca^{2+} content, ER phospholipid depletion and cholesterol accumulation or changes in redox status that occur in diabetes, ER undergoes to a condition of stress that leads to the activation of the Unfolded Protein Response (UPR) (Cnop, Foufelle, and Velloso 2012; Flamment et al. 2012; Hotamisligil 2010). ER stress is defined as an imbalance between the proper folding and secretory capacity of the ER, and the increased load of unfolded proteins, resulting in the accumulation of misfolded proteins. Loss of ER homeostasis activates this ER stress response, which is an adaptive mechanism, especially important in secretory cells, that serves to dynamically expand both the size of the ER and its capacity according to the functional demand placed upon the exocytotic pathway (Cnop, Foufelle, and Velloso 2012).

The primary goal of the UPR is to decrease the unfolded protein load and restore organelle homeostasis. For this purpose, the UPR decreases protein translation and induces transcription of components of the ER machinery involved in folding, N-glycosylation, ER-associated degradation,

quality control, redox homeostasis and lipid biogenesis (Cnop, Foufelle, and Velloso 2012). If these mechanisms of adaptation are insufficient to recover ER homeostasis, cells undergo to apoptosis (Flamment et al. 2012).

The UPR is mediated by three canonical ER stress transducers: PKR-like eukaryotic initiation factor 2a kinase (PERK), inositol-requiring enzyme 1 (IRE1) and activating transcription factor 6 (ATF6). The PERK pathway rapidly attenuates protein translation, whereas the IRE1 and the ATF6 cascades transcriptionally upregulate ER chaperone genes that promote proper folding and ER-associated degradation of proteins, allowing the folding machinery of the ER to reduce the problem of the unfolded proteins.

The three transducers are present in the ER membrane and under non-stressed conditions they are maintained in an inactive state by binding to the immunoglobulin heavy chain binding protein/glucose-regulated protein of 78kDa (BiP/GRP78). BiP is the major ER chaperone and the master regulator of the UPR. During ER stress, BiP is displaced to interact with misfolded luminal proteins; this results in the release of PERK, IRE1 and ATF6, and in their activation (Figure 22).

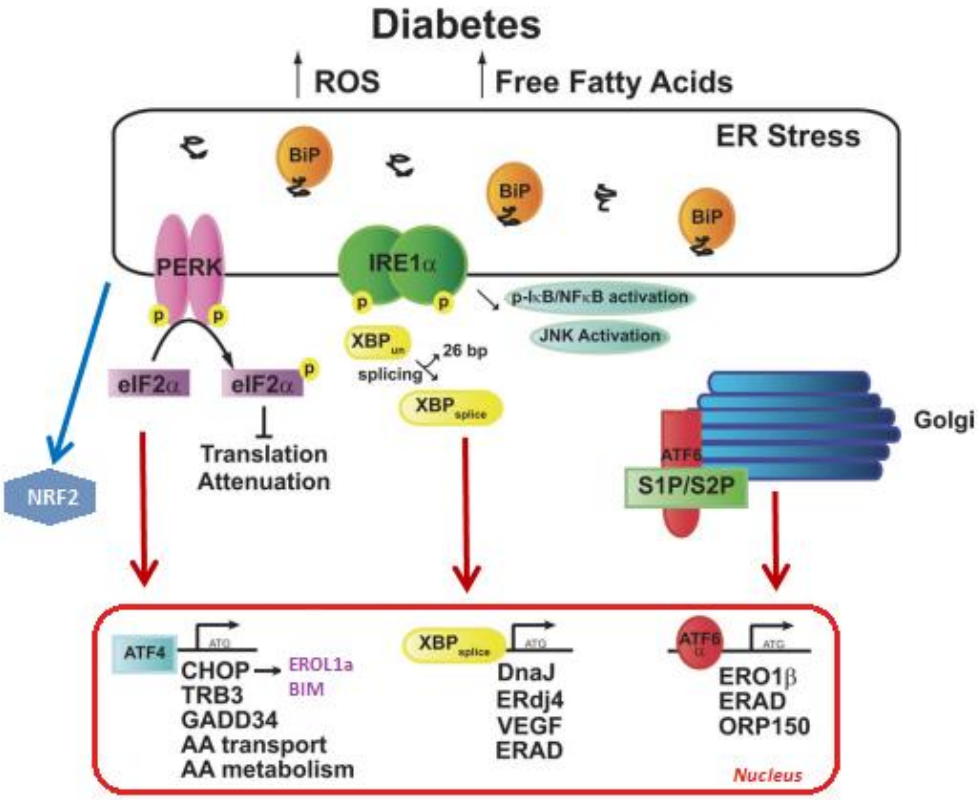

Figure 22: The UPR pathway. In unstressed conditions, BIP chaperone interacts with ATF6, IRE1 and PERK, maintaining them in an inactive state. Upon ER stress, BIP is recruited by unfolded proteins, leading to the activation of the UPR transducers. PERK dimerizes and autophosphorylates, and in turn phosphorylates eIF2a, which induces the selective translation of ATF4. ATF4 regulates the transcription of genes involved in antioxidant response and amino acid transporter synthesis. It also participates in controlling apoptotic pathway through CHOP, a transcription factor that in turn can activate ERO1a and BIM. IRE1, after autophosphorylation, forms the transcription factor XBP1s, which induces expression of ERAD proteins and chaperones. ATF6, once activated by S1P and S2P in the Golgi, transactivates genes encoding ER chaperones and ERAD proteins. Sustained ER stress can lead to ER stress-associated cell death and for this UPR sensors are closely connected to apoptotic pathways (Cunard and Sharma 2011).

PERK is a transmembrane protein with an ER luminal stress-sensing domain, that binds BIP, and a cytosolic kinase domain (Cunard and Sharma 2011). Upon ER stress, PERK phosphorylates the α-subunit of eukaryotic translation initiation factor 2 (eIF2a), leading to rapid reduction in the initiation of mRNA translation, and thus reducing the load of new proteins in the ER. Although general protein translation is inhibited after eIF2a phosphorylation, a subset of genes including the activating transcription factor 4 (ATF4) are preferentially translated (Cunard and Sharma 2011). ATF4 in turn drives the transcription of specific UPR target genes, such as tribbles homolog 3 (TRB3), E-selectin, VEGF, C/EBP homologous protein (CHOP, also known as GADD153) and other important genes involved in amino acid metabolism. PERK also phosphorylates NRF2, involved in the modulation of antioxidant response. By activating the expression of the growth arrest and DNA damage-inducible protein (GADD34) that targets the protein phosphatase 1 (PP1) to eIF2a for dephosphorylation, ATF4 also participates in the retrocontrol of PERK signalling (Hotamisligil 2010).

CHOP is a transcription factor that has traditionally been considered an inducer of apoptosis (Oyadomari and Mori 2004). However, it does not promote apoptosis in all cell types, and CHOP's biological effects may be more dependent on CHOP's heterodimeric partner (Halterman et al. 2010). CHOP can activate ERO1α, an ER oxidase, GADD34, TRB3 and the proapoptotic factor BIM (Puthalakath et al. 2007). CHOP also decreases expression of the pro-survival factor BCL-2 (McCullough et al. 2001).

The IRE1/X box binding protein-1 (XBP-1) pathway is the most evolutionarily conserved of the ER stress pathways (Mori 2009). IRE1 is a membrane-bound serine/threonine kinase with endonuclease activity (Cunard and Sharma 2011). When BiP dissociates from IRE1, it is activated to splice a 26-bp intron from XBP-1. This unconventional splicing event induces a translational frame shift that generates a 371-amino acid highly active transcription factor, the XBP1-sp (Cunard and Sharma 2011). XBP1-sp in turn upregulates the transcription of genes encoding ER chaperones, components of the ERAD machinery and phospholipid biosynthesis. Phospholipid biosynthesis leads to expansion of the ER membrane, a structural hallmark of the UPR. IRE1 also has a nonspecific endoribonuclease activity that is responsible for the degradation of ER-localized mRNAs, a process named regulated IRE1-dependent decay (RIDD) (Tabas and Ron 2011). This mechanism also contributes to the reduction of protein accumulation in the ER. Moreover, IRE1 activates JNK by recruiting the scaffold protein tumor necrosis factor receptor-associated factor 2 (TRAF2) as well as ASK1 and caspase 12, which are pro-apoptotic messengers (Tabas and Ron 2011).

Activation of ATF6 allows its translocation from the ER to the Golgi where it is cleaved by site 1 protease (S1P) and site 2 protease (S2P). The cleaved-off cytoplasmic domain of ATF6 is an active transcription factor that transactivates genes involved in ERAD, lipid biosynthesis, ER expansion and protein folding, including BiP. ATF6 activity is regulated by the Wolfram syndrome 1 (WFS1) protein, which targets ATF6 to the E3 ubiquitin ligase HRD1, resulting in ATF6 ubiquitination and proteasomal degradation (Fonseca et al. 2010).

9.3. Interrelationship between ER stress, diabetes and ROS: the role of NRF2

The growing interest for ER stress in the field of metabolic diseases comes from the pioneering studies of Hotamisligil and coworkers. They showed that UPR markers are overexpressed in the liver and adipose tissue of diabetic rodents (Ozcan et al. 2004), and this was further confirmed in biopsies of T2DM patients (Gregor et al. 2009).

Chronic ER stress and activation of the UPR may also result in the accumulation of ROS that promotes a state of oxidative stress (Cullinan and Diehl 2006). So ROS overproduction and the subsequent development of oxidative stress can be considered the cause and the consequence of ER stress. ROS accumulation is due to the UPR-stimulated upregulation of protein chaperones involved in disulfide bond formation in the ER lumen (Hotamisligil 2010). These chaperones use oxidation/reduction reactions, with molecular oxygen as the final electron recipient. This reduced molecular oxygen accumulates during increased protein folding due to UPR activation and is toxic for the cells (Hotamisligil 2010).

In order to anticipate this increase in ROS production and neutralize toxic species during ER stress, the UPR has evolved developing an antioxidant program via PERK signalling and the activation of one of its direct substrates, the transcription factor NRF2. So PERK signalling, via activation of the NRF2 and others substrates as for example ATF4, engages survival responses, coordinates the convergence of ER stress with oxidative stress signalling, and orchestrates the execution of the ARE-dependent gene transcription program (W. Li and Kong 2009).

As explained before, in unstressed cells NRF2 is maintained in a latent cytoplasmic complex with KEAP1. Under conditions of ER stress, UPR in initiated and PERK activation is reached. PERK-dependent phosphorylation triggers dissociation of NRF2/KEAP1 complexes and allows subsequent NRF2 nuclear import. The mechanism by which oxidative stress promotes the dissociation of NRF2 from KEAP1 remains controversial. One model suggests that NRF2 is phosphorylated by PKC (Huang, Nguyen, and Pickett 2000), and others have showed that NRF2 dissociation from KEAP1 and its subsequent activation are mediated by PI3K (Kang et al. 2002) and/or MAPK (Zipper and Mulcahy 2000).

The identification of NRF2 as a PERK substrate, together with eIF2α, strongly convinces that PERK signalling has pro-survival properties and supports the hypothesis that PERK initiates two independent programs of gene and protein expression (Cullinan and Diehl 2006).

OBJECTIVES

The “incretin effect” phenomenon has been reported to be decreased in T2DM patients (Nauck et al. 1986). Although the physiological mechanisms of this reduction are still unknown, it is suspected that it could be due to: (1) a decrease in the incretin hormone in the plasma, as a result of a reduced secretion, or (2) a reduced action, a phenomenon known as “incretin resistance” (Herzberg-Schäfer, Heni, Stefan, Häring, & Fritsche, 2012). So, it has been postulated that in presence of hyperglycaemia and T2DM, GLP-1 and GIP partially lose their protective actions, and that their receptors could play an important role.

A resistance to GLP-1 actions has been recently shown in pancreatic β-cells of diabetic patients by Xu G. and coworkers (Xu et al. 2007). They also observed that gene expression of incretin receptors is significantly decreased in islets of 90% pancreatectomized hyperglycemic rats (Xu et al. 2007). Consistently, other two independent groups working in different models and cell types have confirmed that high glucose exposure induces the reduction of GLP-1R expression (Green et al. 2012; Mima et al. 2012): Green C.J. et al. showed a reduction on GLP-1R expression in fully differentiated human myocytes cultured under chronic high glucose levels (Green et al. 2012); Mima A. et al. observed a reduction of GLP-1R expression on renal cortex protein extracts of diabetic mice (Mima et al. 2012).

As concern as the endothelium, it has been demonstrated that in T2DM patients, hyperglycaemia induces an endothelial resistance to GLP-1 protective effects, which could be restored improving glucose control (Ceriello et al. 2011).

One of the postulated mechanisms to explain this endothelial resistance to the GLP-1 actions in diabetes is the activation of PKCβ, which is induced by hyperglycaemia. It has been proposed that in the renal cortex of diabetic mice PKCβ activation is able to inhibit GLP-1 protective properties by reducing the expression of its receptor (Mima et al. 2012).

Therefore, the aims of this thesis were:

1. **to study GLP-1R expression in HUVEC cells exposed to chronic high glucose levels and assess how this cellular model is able to respond to GLP-1 acute treatment in terms of oxidative stress, ROS production, antioxidant defense system, proliferation and ER stress;**

2. **to decipher the involvement of PKCβ in the GLP-1R signalling pathway in HUVEC cells exposed to sustained high glucose.**

MATERIALS AND METHODS

1. Biological material

- GLP-1 (7-37), 2',7'-Dichlorofluorescein diacetate, protease inhibitor cocktail and phosphatase inhibitor cocktail (Sigma-Aldrich Química,S.L., Madrid, Spain),
- PKC isoform β specific inhibitor LY 333531 mesylate –Ruboxistaurin (Axon Medchem BV, Groningen The Netherlands),
- Wortmannin (Cayman Chemical, Ann Arbor, MI, USA),
- GLP-1 receptor antibody Ab39072 (Abcam plc, Cambridge, UK),
- AKT1/2 (N-9) antibody (sc-1619) (Santa Cruz Biotechnology, Inc., Heidelberg, Germany),
- PKCβ1(E-3) antibody (sc-8049) (Santa Cruz Biotechnology, Inc., Heidelberg, Germany),
- NRF2 (D1C9) antibody (#8882) (Cell signalling technology),
- LMNB1 antibody (# 9087) (Cell signalling technology),
- Phospho-AKT (Ser473) (Cell signalling technology),
- XP antibody (#4060) (Cell signalling technology),
- Cleaved Caspase3 (Asp175) antibody (#9661s) (Cell signalling technology),
- TUBA antibody (T6074) (Sigma-Aldrich Química,S.L., Madrid, Spain),
- ACTB antibody (A-2066) (Sigma-Aldrich Química,S.L., Madrid, Spain),
- EGM™-2 Bulletkit™ (Lonza Ibérica S.A.U., Barcelona, Spain).

2. Cell culture

In this work Human Umbilical Vein Endothelial Cells (HUVECs) were used as cellular model for the experiments. They were isolated from human umbilical veins and kindly provided by Dr. Maribel Díaz (Hemotherapy-Hemostasis Laboratory, Hospital Clínic, Barcelona). HUVECs were cultured with EGM™-2 Bulletkit™, adding supplemental growth factors: human Epidermal Growth Factor (hEGF), Hydrocortisone, human recombinant Fibroblast Growth Factor-Beta (hFGF-b), Heparin, 2% Fetal Bovine Serum (FBS) and Gentamicin/Amphotericin-B (GA), provided with the media, at 37ºC in a humidified atmosphere with 5% CO_2.

2.1. Preparation of complete growth media

1. Obtain one growth kit from freezer; make sure that the caps of all components.
2. Thaw the components of the growth kit just prior to adding them to the basal medium.
3. Obtain one bottle of Vascular Cell Basal Medium (475 mL) from cold storage.
4. Decontaminate the external surfaces of all growth kit component vials and the basal medium bottle by spraying them with 70% ethanol.
5. Using aseptic technique and working in a laminar flow hood or biosafety cabinet, transfer the volume of each growth kit component, as indicated in the Table 1, to the bottle of basal medium using a separate sterile pipette for each transfer.
6. Tightly cap the bottle of complete growth medium and swirl the contents gently to assure a homogeneous solution. Do not shake forcefully to avoid foaming. Label and date the bottle.
7. Complete growth media should be stored in the dark at 2°C to 8°C (do not freeze). When stored under these conditions, complete growth media is stable for 30 days.

Component	*Volume*	*Final Concentration*
rh-EGF	0.5mL	5ng/mL
Heparin sulfate	0.5mL	0.75Units/mL
Hydrocortisone Hemisuccinate	0.5mL	1µg/mL
Fetal Bovin Serum	10.0 mL	2%
Ascorbic Acid	0.5mL	50µg/mL

Table 1: Supplemental growth factors added to the EGM™-2 Bulletkit™.

2.2. Maintenance protocol

1. Before beginning, pre-warm complete growth media in a 37°C water bath. This will take between 10 and 30 minutes, depending on the volume. If using a small volume of medium (50 mL or less), warm only the volume needed in a sterile conical tube. Avoid warming complete growth media multiple times.
2. 24 hours after seeding, remove the cells from the incubator and view each flask under the microscope to determine percent cellular confluence.
3. Carefully remove the spent media without disturbing the monolayer.
4. Add 5 mL of fresh, pre-warmed complete growth media per 25 cm^2 of surface area and return the flasks to the incubator.
5. After 24 to 48 hours, view each flask under the microscope to determine percent cellular confluence. When cultures have reached approximately 80% confluence and are actively proliferating (many mitotic figures are visible), they can be subcultured.

2.3. Subculturing protocol

We followed the instructions for a 25 cm^2 flask. We adjusted all volumes accordingly for other size flasks.

1. Passage normal HUVECs when culture has reached approximately 80% confluence.
2. Warm both the Trypsin-EDTA and the Trypsin Neutralizing Solution, consisting in the medium, to room temperature prior to dissociation. Warm complete growth medium to 37°C prior to use with the cells.
3. Aspirate the spent media without disturbing the monolayer.
4. Rinse the cell layer two times with 3 to 5 mL DPBS to remove residual traces of serum.
5. Add 1.5mL trypsin EDTA solution.
6. Gently rock each flask to ensure complete coverage of the trypsin EDTA solution over the cells, and then aspirate the excess fluid off of the monolayer.
7. Observe the cells under the microscope. When the cells pull away from each other and round up (typically within 3 to 5 minutes), remove the flask from the microscope and gently tap it from several sides to promote detachment of the cells from the flask surface.
8. When the majority of cells appear to have detached, quickly add an equal volume of Trypsin Neutralizing Solution. Gently pipette or swirl the culture to ensure all of the Trypsin-EDTA solution has been neutralized.
9. Transfer the dissociated cells to a sterile centrifuge tube and set aside while processing any remaining cells in the flask.

10. Add 3 to 5 mL Dulbecco's Phosphate-Buffered Saline (DPBS) to the flask to collect any additional cells that might have been left behind.
11. Transfer the cell/DPBS suspension to the centrifuge tube containing the trypsin EDTA dissociated cells.
12. Repeat steps 10 and 11 as needed until all cells have been collected from the flask.
13. Centrifuge the cells at 1000 RPM for 5 minutes.
14. Aspirate the neutralized dissociation solution from the cell pellet and resuspend the cells in 4mL of growth medium and note the total volume of the total volume of the diluted cell suspension.
15. Determine cell count and viability using Trypan Blue exclusion Dye. The Trypan blue is a vital stain used to selectively color dead tissues or cells blue. It is a diazo dye. Live cells or tissues with intact cell membranes are not colored. Since cells are very selective in the compounds that pass through the membrane, in a viable cell Trypan blue is not absorbed; however, it traverses the membrane in a dead cell. Hence, dead cells are shown as a distinctive blue color under a microscope.
16. Use the following equation to determine the total number of viable cells.

$$\text{Total of Viable Cells} = \frac{\text{Total cell count X \% viability}}{100}$$

17. Determine the total number of flasks to inoculate by using the following equation. The number of flasks needed depends upon cell yield and seeding density. If seeding into well plates at this time the recommended density is 10.000 cells/cm².

$$\text{Total of flasks to inoculate} = \frac{\text{Total \# of viable cells}}{\text{Growth area X Rec. Seeding Density}}$$

18. Use the following equation to calculate the volume of cell suspension to seed into your flasks.

$$\text{Seeding Volume} = \frac{\text{Total volume of diluted cell suspension}}{\text{\# flasks as determined in step 17}}$$

19. Prepare flasks by labelling each flask with the passage number, strain number, cell type and date.
20. Carefully transfer growth medium to new culture vessels adding 1mL growth medium for every 5cm² surface area of the flask (1mL/5cm²).
21. After mixing the diluted cells with 5mL pipet to ensure a uniform suspension, dispense the calculated volume into the prepared subculture flasks.

2.4. Cryopreservation and recovery

Special attention is needed to cryopreserve and thaw primary cells, in order to minimize cell damage and death during each process. Cryopreservation of human cells is best achieved with the use of a cryoprotectant, such as Dimethyl sulfoxide (DMSO) or glycerol. HUVEC cells were

cryopreserved in a mixture of 80% complete growth medium supplemented with 10% FBS and 10% DMSO. The freezing process was performed in a progressive manner at a rate of -1°C per minute, to minimize the formation of ice crystal within the cells. Once frozen, cultures were stored in the vapor phase of liquid nitrogen.

Thawing cryopreserved cells is a rapid process and it was accomplished by immersing frozen cells in a 37 °C water bath for about 1 to 2 minutes. Care should be taken not centrifuge primary cells upon thaw, since they are extremely sensitive to damage during recovery from cryopreservation. It is best to plate cells directly upon thaw, and allow cultures to attach for the first 24 hours before changing the medium to remove residual DMSO.

3. Experimental design

Cells were grown at $1.2x10^5$ in 6-well plates or at $2x10^6$ in $100mm^2$ dishes. HUVECs were cultured in normal glucose (NG) (5mmol/L) or high glucose (HG) (25mmol/L) during 21 days, changing the media each 48 hours and without passaging the cells. After this period, Wortmannin was added overnight to the media at 1µM, and GLP-1(7-37) or Ruboxistaurin were added at 50nM or 0.5µM, respectively, alone or in combination 1 hour before cell harvesting.

All the experiments were performed in duplicate between 4 and 7 cell passages.

4. RNA isolation and qRT-PCR

Total RNA was isolated from HUVECs using Total RNA isolation kit (Norgen Biotek Corp, Thorold, Ontario, Canada). First-strand cDNA was prepared using 1-2ug of total RNA, the Superscript III RT kit and random hexamer primers (Invitrogen, Carlsbad, CA, USA) in a total volume of 25 µl according to the manufacturer's instructions. Reverse transcription reaction was carried for 90min at 50ºC and an additional 10min at 55ºC. Real time PCR (qRT-PCR) was performed on an ABI Prism 7900 sequence detection system using SybrGreen reagents (Takara Bio Company, Clontech, Mountain View, CA, USA) and TaqMan® Gene Expression Master Mix (Life Technologies, Madrid, Spain).

4.1. RNA Extraction protocol

Purification is based on spin column chromatography using Norgen's proprietary resin as the separation matrix. The RNA is preferentially purified from other cellular components such as proteins without the use of phenol or chloroform. The process involves first lysing the cells or tissue of interest with the provided Lysis Solution. Ethanol is then added to the lysate, and the solution is loaded onto a spin-column. Norgen's resin binds RNA in a manner that depends on ionic concentrations. Thus only the RNA will bind to the column, while the contaminating proteins will be removed in the flowthrough or retained on the top of the resin. The bound RNA is then washed with the provided Wash Solution in order to remove any remaining impurities, and the purified total RNA is eluted with the Elution Solution.

1. Cell lysate preparation
    a. Aspirate media and wash cell monolayer with an appropriate amount of PBS. Aspirate PBS.
    b. Add 350 µL of Lysis Solution directly to culture plate.
    c. Lyse cells by gently tapping culture dish and swirling buffer around plate surface for five minutes.
    d. Transfer lysate to a microcentrifuge tube.
    e. Add 200 µL of 95 – 100% ethanol to the lysate. Mix by vortexing for 10 seconds.

2. Binding RNA to column
    a. Assemble a column with one of the provided collection tubes.
    b. Apply up to 600 µL of the lysate with the ethanol (from Step 1) onto the column and centrifuge for 1 minute.
    c. Discard the flowthrough. Reassemble the spin column with its collection tube.
    d. Depending on your lysate volume, repeat Step 2b and 2c as necessary.

3. Column wash
    a. Apply 400 µL of Wash Solution to the column and centrifuge for 1 minute.
    b. Discard the flowthrough and reassemble the spin column with its collection tube.
    c. Repeat steps 3a and 3b to wash column a second time.
    d. Wash column a third time by adding another 400 µL of Wash Solution and centrifuging for 1 minute.
    e. Discard the flowthrough and reassemble the spin column with its collection tube.
    f. Spin the column for 2 minutes in order to thoroughly dry the resin. Discard the collection tube.

4. RNA elution
    a. Place the column into a fresh 1.7 mL Elution tube provided with the kit.
    b. Add 50 µL of Elution Solution to the column.
    c. Centrifuge for 2 minutes at 200 x g (~2,000 RPM), followed by 1 minute at 14,000 x g.

5. Storage of RNA
    The purified RNA sample may be stored at –20°C for a few days. It is recommended that samples be placed at –70°C for long term storage.

4.2. RNA quantification

For each sample, 1 µl total RNA was quantified. Total RNA concentrations were quantified using the NanoDrop® ND-100 Spectrophotometer and ND-1000 v3.1.0 (Labtech International Ltd, Lewes, East Sussex, U.K.).

1. Before starting the software module, clean the sample surfaces with DI water to remove any dried sample that might be present.
2. Open the Nanodrop program and the appropriate module (e.g., RNA).

3. Wipe off the top and bottom sensors of the instrument with a Kimwipe. These are just the polished ends of fiber optic cable, so wiping is sufficient to prevent carryover.
4. Pipette 2 µL of DD water (stored in a blue microtube) onto the sensor.
5. Wipe the sensors and pipette on 2 µL of the corresponding blank (Buffer EB or whatever solution your prep is in).
6. Wipe the sensors and pipette on 2 µL of your sample.
7. Click Measure and record the concentration measured.
8. For DNA, the peak should be at 260 nm, and as a general rule, the 260/280 ratio should be between 1.8 and 2.0.

4.3. DNase treatment of extracted total RNA

In order to remove any contaminating DNA, extracted total RNA was treated with DNase using Deoxyribonuclease I, Amplification Grade (DNase I Amp Grade) (Invitrogen, Carlsbad, CA, USA) according manufactures' instructions. DNase I Amp Grade digests single-and double-stranded DNA to oligodeoxy-ribonucleotides containing a 5'- phosphate. It is suitable for eliminating DNA during critical RNA purification procedures such as those prior to RNA-PCR amplification.

1. Preparation of RNA Sample Prior to RT-PCR. Add the following components to an RNase-free 0.5-ml microcentrifuge tube on ice:
   I. RNA sample 1 µg
   II. 10X DNase I Reaction Buffer 1 µl
   III. DNase I, Amp Grade, 1 U/µl 1 µl
   IV. DEPC-treated water to 10 µl
2. Incubate tube(s) for 15 min at room temperature.
3. Inactivate the DNase I by the addition of 1 µl of 25 mM EDTA solution to the reaction.
4. Heat for 10 min at 65°C.
5. The RNA sample is ready to use in reverse transcription, prior to amplification.

4.4. Retrotrascription of mRNA into cDNA

In order to remove any contaminating DNA, extracted total RNA was treated with the Superscript III RT kit and random hexamer primers (Invitrogen, Carlsbad, CA, USA) in a total volume of 25 µl according to the manufacturer's instructions.

1. First-Strand cDNA synthesis
   a. Add 50ng of random hexamer primers to a nuclease-free microcentrifuge tube.
   b. Heat mixture to 65°C for 5 minutes and incubate on ice for at least 1 minute.
   c. Collect the contents of the tube by brief centrifugation and add:
      I. 5X First-Strand Buffer 4 µl
      II. 0.1 M DTT 1 µl
      III. RNaseOUT™ Recombinant RNase Inhibitor (40 units/µl) 1 µl
      IV. SuperScript™ III RT (200 units/µl) 1 µl
   d. Mix by pipetting gently up and down. If using random primers, incubate tube at 25°C for 5 minutes.

e. Incubate at 50°C for 30–60 minutes. Increase the reaction temperature to 55°C for gene-specific primer. Reaction temperature may also be increased to 55°C for difficult templates or templates with high secondary structure.
f. Inactivate the reaction by heating at 70°C for 15 minutes. The cDNA can now be used as a template for amplification in PCR. However, amplification of some PCR targets (those >1 kb) may require the removal of RNA complementary to the cDNA. To remove RNA complementary to the cDNA, add 1 µl (2 units) of E. coli RNase H and incubate at 37°C for 20 minutes.

2. PCR Reaction
The following example reaction is recommended as a starting point:
a. Add the following to a PCR reaction tube:

I. 10X PCR Buffer [200 mM Tris-HCl (pH 8.4), 500 mM KCl]	5 µl
II. 50 mM MgCl2*	1.5 µl
III. 10 mM dNTP Mix	1 µl
IV. Sense primer (10 µM)	1 µl
V. Antisense primer (10 µM)	1 µl
VI. Taq DNA polymerase (5 U/µl)	0.4 µl
VII. cDNA (from first-strand reaction)	2 µl
VIII. Autoclaved, distilled water	to 50 µl

b. Mix gently and layer 1–2 drops (~50 µl) of silicone oil over the reaction.
c. Heat reaction to 94°C for 2 minutes to denature.
d. Perform 15–40 cycles of PCR. Annealing and extension conditions are primer and template dependent and must be determined empirically.

3. Storage of cDNA
cDNAs were stored at -20ºC for downstream applications.

4.5. Quantitative PCR (real-time RT-PCR)

Unlike conventional PCR, where the product of the reaction is detected at its end, real-time RT-PCR allows quantification of the desired product at any point of the amplification process. In other terms, the amplified DNA is detected as the reaction progresses in "real time".

There are different ways to follow the amplification and all of them are based on measuring fluorescence so that the more amplification of the transcript we have the more fluorescence signal we observe. Two common methods for the detection of products are the non-specific fluorescent dyes that intercalate with any double-stranded DNA (SybrGreen® fluorophore), and sequence-specific DNA probes consisting of oligonucleotides that are labeled with a fluorescent reporter which allows detection only after hybridization of the probe with its complementary sequence (TaqMan®). Double-strand DNA (dsDNA) dyes such as SybrGreen® bind all dsDNA PCR products, including non-specific PCR products, while specific fluorescent reporter probe such as TaqMan® prevent the detection of this kind of non-specific PCR products.

In this work we used both methods, as explained below.

4.5.1. SybrGreen® Real-Time RT-PCR

This method uses a DNA intercalator, the SybrGreen® fluorophore, that emits fluorescence when bound to ds DNA. Monitoring fluorescence allows for quantification of amplified products. Measuring the fluorescence intensity also provides the melting temperature of amplified DNA. The premixed reagent contains Tli RNase H, a heat-resistant RNase H that minimizes PCR inhibition by degrading residual mRNA when using cDNA as template.

Each multiplex reaction was of 10 µl volume, consisting of (Table 2):

Components	*µl*
SYBR Premix Ex Taq (2X)	5
PCR Forward Primer (10uM)	0,25
PCR Reverse Primer (10uM)	0,25
ROX Reference Dye	0,2
cDNA (10ng)	2
RFW	2,3
Final Volum	**10**

Table 2: SybrGreen® Real-Time RT-PCR

4.5.2. TaqMan® Real-Time RT-PCR

Real-time RT-PCR quantitation of samples was carried out via a two-step RT-PCR assay utilising TaqMan® Gene Expression Assays (Applied Biosystems):

1. in the reverse transcription (RT) step, cDNA is reverse transcribed from RNA;
2. in the PCR step, PCR products are quantitatively synthesized from cDNA samples using the TaqMan Gene Expression Master Mix.

Prior to real-time RT-PCR reactions, an efficiency assay was performed for each gene of interest. Serial dilutions of pooled, neat cDNAs were set up in singleplex and multiplex reactions to determine whether the gene of interest amplified with equal efficiency to that of a reference/housekeeping gene [β-actin (ACTB) or glyceraldehyde 3-phosphate dehydrogenase (GAPDH)].

Efficiencies, as calculated according to the manufacturer's instructions (ABI PRISM® 7700 Sequence Detection System - SDS - User Bulletin), were considered to be equal if the absolute value of the slope was < 0.1. Following efficiency tests, multiplex reactions were carried out for genes of interest reacting with similar efficiency to a reference gene.

Each multiplex reaction was of 5 µl volume, consisting of (Table 3):

Components	*µl*
TaqMan® Universal Master Mix	2,5
20X Target Primers	0,25
cDNA (10ng)	2
RNase free water	0,25
Final Volum	**5**

Table 3: TaqMan® Real-Time RT-PCR

4.5.3. Quantification and gene expression analysis

Reactions were carried out in barcoded 384-well plates. For genes of interest with relative efficiencies dissimilar to those of reference genes, reactions were carried out in singleplex (with equal volumes of nuclease-free water in place of the relevant probe) but within the same plate.

The *2-ΔΔCt comparative method* was used for the relative quantitation of gene expression according to the manufacturer's instructions (ABI PRISM® 7700 Sequence Detection System User Bulletin). It is a common employed method of quantification that relies on plotting florescence against the number of cycle on a logarithmic scale. When the amplification reaches a certain level of florescence detection (threshold), it is considered that the gene starts to be expressed. The number of cycles at which the reporter florescence is greater than the threshold, is considered the Ct of the gene (threshold cycle).

In order to establish the threshold for each gene, an algorithm is automatically executed by the SDS Program (Sequence Detection System, Applied Biosystems), which sets a point on the region of exponential amplification between the background signal and the saturation level.

Regarding the normalization of the quantification, the expression the housekeeping gene, that is homogenously expressed in our samples, was used. This control gene allows the normalization between different samples and the quantification is expressed as ratio of the specific gene respect to the control gene.

5. Extraction and quantification of proteins

Briefly, for protein analysis HUVECs were lysed in RIPA Buffer (Sigma-Aldrich) adding 10% proteases and 1% phosphatases inhibitors (Sigma-Aldrich Química, S.L., Madrid, Spain). 50µg of lysates were separated by electrophoresis using PAGEr gels (4-12%) (Lonza Ibérica S.A.U., Barcelona, Spain) and transferred to a Polyscreen PVDF membrane (Perkin Elmer, Waltham, MA, USA). The membranes were then incubated with the appropriate secondary horseradish peroxidase-conjugated IgG antibodies (GE Healthcare Europe GmbH, Barcelona, Spain) at a 1:3,000 dilution for 1 h at room temperature. Blots were visualized with ECL Reagent (Pierce Biotechnology, Rockford, IL, USA) using a LAS4000 Lumi-Imager (Fuji Photo Film, Valhalla, NY, USA). Protein spots were quantitated with Image J software (http://rsb.info.nih.gov/ij/index.html). β-actin or α-tubulin served as the loading control. Protein content was determined using Bradford Assay Buffer (Sigma-Aldrich Química, S.L., Madrid, Spain).

5.1. Protein Extraction

Proteins were routinely extracted from HUVECs at passages between 4 and 7, grown in 6-well plates. After the period of 21 days and the specific treatment with Wortmannin, GLP-1(7-37) and/or Ruboxistaurin, medium was removed and cells were washed with PBS (Sigma-Aldrich Química, S.L., Madrid, Spain) and consequently lysed in 100 µl of RIPA Buffer, consisting of:

- 50 mM Tris-HCl (pH 7.4),
- 150 mM NaCl,
- 1% NP-40,
- 0,25% Na-deoxycholate,

- Protease Inhibitor Mix,
- SDS 0,1%.

At RIPA Buffer 10% proteases and 1% phosphatases inhibitors were added.

Cells were gently scraped off the bottom of the plate into the buffer and transferred to a microcentrifuge tube.

The method used for disrupting membrane lipid bilayer and allow the out of the proteins was the sonication. Tubes with the collected cells were briefly vortexed and proceed to sonication by using the Bioruptor® with the following settings:

- power: H (High) position;
- sonication cycle: 30 sec ON/59 sec OFF;
- total sonication time: 2 cycles;
- temperature: 4°C.

After sonication, the extracted proteins were centrifuged at 14,000 rpm for 15 min. The supernatant was transferred to a new tube and stored at -20ºC until required.

5.2. Determination of protein concentration

Protein concentration was determined using the Bradford Protein Assay kit (Thermo Scientific, Waltham, MA, USA) according to the manufacturer's instructions. Bradford Assay is a colorimetric protein assay, based on an absorbance shift of the dye Coomassie Brilliant Blue G-250: when the dye binds protein in an acidic medium, an immediate shift in absorption maximum occurs from 465 nm to 595 nm with a concomitant color change from brown to blue.

Assays were performed in 96-well plates according the protocol below:

1. Pipette 5 µl of each standard or unknown sample into the appropriate microplate wells.
2. Add 250 µl of the Coomassie Plus Reagent to each well and mix with plate shaker for 30 seconds.
3. Remove plate from shaker. For the most consistent results, incubate plate for 10 minutes at room temperature.
4. Measure the absorbance at or near 595 nm on a plate reader.
5. Subtract the average 595 nm measurement for the Blank replicates from the 595nm measurements of all other individual standard and unknown sample replicates.
6. Prepare a standard curve by plotting the average Blank-corrected 595 nm measurement for each bovine serum albumin (BSA) standard versus its known concentration (µg/µl).

Protein concentrations were estimated by reference to absorbances obtained for the series of standard protein dilutions, which are assayed alongside the unknown samples. Dilutions of a BSA protein standard ranging from 2,0 µg/µl – 0,25 µg/µl were made in distilled H_20 and used to generate a standard curve for each assay.

Absorbance at 595 nm was determined for all wells using a Wallac Victor2 plate reader (Wallac, Turku, Finland). Both samples and standards were measured in duplicate and an average value calculated.

5.3. Western Blot assessment

Western blot is a widely used analytical technique to detect specific proteins in a sample of tissue homogenate or cellular extracts. It uses polyacrylamide gel electrophoresis (PAGE) to separate denatured proteins by the length of the polypeptide. The proteins are then transferred to a membrane (typically nitrocellulose or PVDF), where they are stained with specific antibodies to the target protein. Thus, the immobilized proteins are detectable by immunological procedures: the membrane is incubated with a first antibody directed against the protein and with second antibodies that are directed against the first and to which an enzyme is covalently linked. A color reaction carried out by the enzyme will indicate the position of the protein.

50µg of lysates were mixed with LDS Sample Loading Buffer 4X (Thermo Scientific, Waltham, MA, USA), that is a non-reducing lithium dodecyl sulfate sample loading buffer. After mixture, lysates were denatured by incubating them for 5 minutes at 95ºC. Proteins were then resolved using PAGEr gels (4-12%). Proteins were transferred onto a Polyscreen PVDF membrane during 1 hour at 350mA in Transfer Buffer (Lonza Ibérica S.A.U., Barcelona, Spain), according manufacture's instructions. Membranes were then blocked with shaking in TBS-T [150 mM NaCl, 50 mM Tris, 0.1% (v/v) Tween-20] + 5% (w/v) BSA powder (Blocking Buffer) for approximately 1 hour before overnight incubation at 4ºC with shaking in a primary antibody solution. Primary antibodies were diluted to appropriate concentrations in Blocking Buffer. Membranes were then washed 3 times in TBS-T at room temperature with each wash lasting approximately 10 minutes. Secondary antibodies were also diluted in Blocking Buffer and incubated with membranes at room temperature for 2 hours with shaking. A further three 10 minute washes in TBS-T were then performed.

Proteins were visualized with ECL Reagent according the manufacturer's instructions, using a LAS4000 Lumi-Imager. Blots were exposed for varying lengths of time, ranging from 10 seconds to 2-5 minutes. Protein spots were quantitated with Image J software and β-actin or α-tubulin served as the loading control.

5.4. Stripping

Stripping is the term used to describe the removal of primary and secondary antibodies from a western blot membrane. Stripping is useful to investigate more than one protein on the same blot, for instance a protein of interest and a loading control. The stripping and re-probing a single membrane instead of running and blotting multiple gels have the advantage of saving samples, materials and time.

For our experiments, we used the follow stripping solution, composed of:

- Tris-aminomethane (0.5 M pH 6.8) (Sigma-Aldrich Química, S.L., Madrid, Spain),
- SDS 10% (Sigma-Aldrich Química, S.L., Madrid, Spain),
- β-mercaptoetanol (Sigma-Aldrich Química, S.L., Madrid, Spain)**.**

This was the protocol we followed:

1. Warm the buffer to 50°C in bath-water.
2. Add the buffer to a small plastic box which has a tight lid. Use a volume that will cover the membrane.
3. Add the membrane. Incubate at 50°C for up to 45 minutes with some agitation.
4. Dispose of the solution as required for β-mercaptoethanol based buffers.
5. Rinse the membrane under running water tap for 1-2 hours.

6. Traces of β-mercaptoethanol will damage the antibodies. Wash extensively for 5 minutes in TBS-T.
7. The membrane is now ready for re-blocking stage.

6. Nuclear and cytoplasm fractionation

Subcellular localization is crucial for the study of proper function of a protein. Deregulation of subcellular localization may lead to pathological consequences resulting in diseases like cancer, diabetes. Immuno-fluorescent staining and subcellular fractionation can be used to determine localization of a protein. Subcellular fractionation consists into separate the nuclear, cytosolic, and membrane fractions of cultured cell lines using a centrifuge and ultracentrifuge. The fractions can be further analysed using western blot.

For our studies, we used a protocol that allowed us to separate nucleus and cytoplasm fractions. Cells were grown in 100mm^2 dishes. After 21 days in NG/HG culture and treatments addition, HUVECs were lysed with buffer A (10mM Tris-Hcl PH 7.8, 1% Igepal, 10mM β-mercaptoethanol, 10% protease inhibitor cocktail and 10% phosphatase inhibitor cocktail). An equal volume of H_2O was added to cells. Shear cells were collected using a 25-G gauge needle and nuclei recovered by centrifugation at 3000rpm for 10 minutes. Nuclei were washed with 200 µl buffer B (10mM Tris-Hcl PH 7.4, 2mM MgCl2, 10% protease inhibitor cocktail and 10% phosphatase inhibitor cocktail), centrifuged at 3000rpm for 10 minutes and then suspend in 70 µl RIPA buffer with proteases and phosphatases inhibitors. After 10 minutes on ice, nuclei were disrupted using 27-G gauge needle.

After separation and collection, for nuclei and cytoplasm a protein extraction was performed, as explained before (see paragraph 5.1.). Then the proteins were quantified (see paragraph 5.2.) and analysed for fester blot (see paragraph 5.3.). Internal loading control was used to make sure each fraction did not cross-contaminate others. Also relative amount were determined between samples to ensure equal loading. For example, α-tubulin was used for the cytosolic fraction, while laminin-β1 was used for the nuclear fraction. α-tubulin and laminin-β1 were tested after protein was transferred onto a PVDF membrane.

7. Proliferation and cell viability assay

Assays to measure proliferation, viability and cytotoxicity are commonly used to monitor the response and health of cells in culture after treatment with various stimuli. Cell-based assays also are widely used for measuring receptor binding and a variety of signal transduction events that may involve the expression of genetic reporters, trafficking of cellular components or monitoring organelle function.

The proper choice of an assay method depends on the number and type of cells used as well as the expected outcome. Assays for cell proliferation may monitor the number of cells over time, the number of cellular divisions, metabolic activity or DNA synthesis. There are a variety of assay methods that can be used to estimate the number of viable eukaryotic cells.

7.1. MTT assay

MTT (3-[4,5-dimethylthiazol-2-yl]-2,5- diphenyltetrazolium bromide; thiazolyl blue) assay was the first homogeneous cell viability assay developed for a 96-well format that was suitable for high throughput screening. The MTT tetrazolium assay technology has been widely adopted and remains popular in academic world as evidenced by thousands of published articles.

MTT tetrazolium reduction is a water soluble tetrazolium salt yielding a yellowish solution when prepared in media or salt solutions lacking phenol red. Dissolved MTT is converted to an insoluble purple formazan by cleavage of the tetrazolium ring by dehydrogenase enzymes. This water insoluble formazan can be solubilized using isopropanol or other solvents and the dissolved material is measured spectrophotometrically yielding absorbance as a function of concentration of converted dye. Viable cells with active metabolism convert MTT into a purple colored formazan product with an absorbance maximum near 570 nm. When cells die, they lose the ability to convert MTT into formazan, thus color formation serves as a useful and convenient marker of only the viable cells.

In our experiments we dissolved the MTT powder (Sigma-Aldrich Química, S.L., Madrid, Spain) in distilled H_20. The solution was then filtered through a 0.2 µm filter and stored at 2–8 °C for frequent use or frozen for extended periods. Routinely, MTT stock solution (5 mg/ml) is added to each culture at the final concentration of 0.2 mg/ml incubated for 4 hours. At the end of the incubation period the medium was removed and the converted dye was solubilized with acidic isopropanol.

The quantity of formazan, presumably directly proportional to the number of viable cells, was measured by recording changes in absorbance at 570nm using the plate reading spectrophotometer. A reference wavelength of 630nm was used.

7.2. 5-bromodeoxyuridine (BrdU) incorporation assay

BrdU incorporation was assayed using the Cell Proliferation ELISA (BrdU) colorimetric assay (Roche, Mannheim, Germany) according to the manufacturer's instructions. Briefly, HUVECs were grown at $2.5x10^3$ at 96 well-plate and cultured in normal glucose or high glucose during 21 days, changing the media each 48h. After this period, GLP-1(7-37) or Ruboxistaurin were added at 50nM or 0.5µM, respectively, alone or in combination 1h before overnight cell labeling with BrdU, fixed, and washed. Anti-BrdU-POD working solution and substrate solution were added, and BrdU incorporation was quantified by measuring the absorbance at 370 nM in a microplate reader (Synergy HT, BioTek BioTek Instruments, Inc., Winooski, Vermont, USA).

8. ROS measurement

The fluorescent probe, 2',7'-Dichlorofluorescein diacetate (H_2DCFDA), was used to measure the intracellular generation of ROS. $5x10^4$ HUVEC were grown in clear flat bottom treated 96-well plates during 21 days under NG or HG conditions. At the end of the experiment cells were treated with indicated drugs and the reactions were stopped by removing the media and staining cells with 20 µM H_2DCFDA for 30 min at 37°C. The fluorescence intensity of H_2DCFDA was kinetically measured at an excitation and emission wavelength of 485 nm and 530 nm for H_2DCFDA using a fluorescent microplate reader (Synergy HT, BioTek BioTek Instruments, Inc., Winooski, Vermont, USA).

9. Immunofluorescence characterization of HUVECs

As explained in the paragraph 2 of this section, HUVEC cells at passage 5 were plated onto sterile coverslips in 8 well plates. 24 hours later medium was removed and normal glucose or high glucose treatment during 21 days was started, changing the media each 48 hours and without passaging the cells. After this period, Wortmannin was added overnight to the media at 1μM, and GLP-1(7-37) or Ruboxistaurin were added at 50nM or 0.5μM, respectively, alone or in combination 1 hour before cell harvesting.

At the end of different treatments, cells were washed twice with ice-cold PBS and consequently fixed in 4% paraformaldehyde for 5 minutes at room temperature. They were then permeabilized in PBST for 30 minutes at room temperature and blocked in 2% BSA in PBST for 1 hour at room temperature. Cells were washed twice more in PBS and then incubated with the appropriate primary antibody (1:50 for anti-GLP-1R and 1:50 for PKCβ, both in 20% goat serum/PBS) at room temperature for 30 minutes. This passage was followed by 3 washes in PBS. Cells were then incubated with goat-anti-mouse IgG-fluoroscein isothiocyanate (FITC – green fluorescence) for GLP-1R immunoloablling or Tetramethylrhodamine (TRITC – red fluorescence) conjugate (Dako) secondary antibody (1:200 in 20% goat serum/PBS) for 30 minutes at room temperature and washed a further 3 times in PBS. The nuclei were immunolabeled with Hoechst (blue fluorescence). Cell-free sides of coverslips were subsequently washed with dH_2O, coverslips mounted in Vectashield (Vector Laboratories Inc., Burlingame, CA, U.S.A.) and finally cells were visualized under a Zeiss laser scanning confocal microscope.

10. Statistical analysis

All values are represented as means ± standard error of the mean (SEM). For comparisons of a continuous variable in data sets with more than 2 groups, One-way analysis of variance (ANOVA) using GraphPad Prism 5 (GraphPad Software, Inc., La Jolla, CA, USA.) was applied to determine statistical significance among groups, followed by the Tukey's post-hoc test for all possible pairwise comparisons. Also the two-tailed Student's t-test to validate the significance between groups.

A P-value of less than 0.05 (two tailed) was considered significant.